Synthesis and structures of transition metal pacman complexes of heteroditopic Schiff-base pyrrole macrocycles

Post-print of a peer-reviewed article published by the Royal Society of Chemistry.
Published article available at: http://dx.doi.org/10.1039/C2DT31850D

Cite as:
Leeland, J. W., Finn, C., Escuyer, B., Kawaguchi, H., Nichol, G. S., Slawin, A. M. Z., & Love, J. B. (2012). Synthesis and structures of transition metal pacman complexes of heteroditopic Schiff-base pyrrole macrocycles. *Dalton Transactions*, 41(45), 13815-13831.

Manuscript received: 13/08/2012; Accepted: 05/09/2012; Article published: 01/10/2012

Synthesis and Structures of Transition Metal Pacman Complexes of Heteroditopic Schiff-Base Pyrrole Macrocycles**

James W. Leeland,[1] Colin Finn,[1] Bérengère Escuyer,[2] Hiroyuki Kawaguchi,[3] Gary S. Nichol,[1] Alexandra M. Z. Slawin[4] and Jason B. Love[1,*]

[1]EaStCHEM, School of Chemistry, Joseph Black Building, University of Edinburgh, West Mains Road, Edinburgh, EH9 3JJ, UK.

[2]Ecole Nationale de Chimie, Physique et Biologie, Lycée Pierre Gilles de Gennes, 11 rue Pirandello, 75013 Paris, France.

[3]Department of Chemistry, Tokyo Institute of Technology, 2-12-1 Ookayama, Tokyo 152-8550, Japan.

[4]EaStCHEM School of Chemistry, University of St. Andrews, North Haugh, St. Andrews, Fife, UK.

[*]Corresponding author; e-mail: jason.love@ed.ac.uk, fax: +44 (0)131 6504743, tel: +44 (0)131 6504762

[**]The authors thank the EPSRC(UK), the Japanese Society for the Promotion of Science (JWL, to work in the laboratories of Prof. Kawaguchi), ENCPB Pierre Gilles de Gennes (internship for BE), the University of Edinburgh, and EaStCHEM for their support.

[†]Dedicated to Professor David Cole-Hamilton on the occasion of his retirement and for his outstanding contribution to transition metal catalysis.

Supporting information:
[‡]Electronic supplementary information (ESI) available: Crystallographic data and the X-ray crystal structure of $Mn_2(^{2+2}L^P)$. CCDC 895814–895827. For ESI and crystallographic data in CIF or other electronic format see http://dx.doi.org/10.1039/C2DT31850D

Graphical abstract:

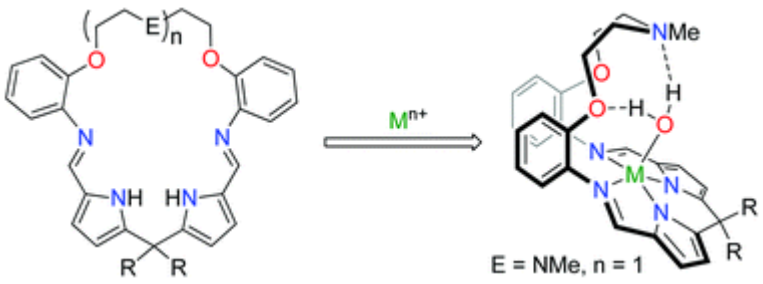

Abstract

A series of polydentate dual-compartment, Schiff-base pyrrole macrocycles has been prepared through the straightforward Lewis acid catalysed [1+1] condensation reactions between ONO or O_5-linked aryldiamines and dipyrromethane dialdehydes. These macrocycles display hydrogen-bond acceptor and donor properties and provide distinct N_4 and O_5/ONO donor sets for metallation reactions, so forming alkali, alkaline earth, and transition metal complexes that were characterised spectroscopically and crystallographically. While the conformationally flexible O_5 donor set allows the formation of helical potassium salt structures, the transition metal complexes of all variants of these macrocycles invariably adopt wedged, Pacman-shaped structures in which the metal is bound in the pyrrole-imine N_4 donor set, so leaving the ONO/O_5 donor set pendant and apical. In some cases (V, Cr, and Co), this proximate combination of Lewis acid binding site and hydrogen bond acceptor facilitates the coordination of water within the molecular cleft; alternatively, direct interaction between the pendant arm and the metal is seen (*e.g.* Ti). Higher order [2+2] macrocycles were also prepared as minor, inseparable by-products of cyclisation, and Fe_2, Mn_2, and Co_2 complexes of these larger macrocycles were found to adopt binuclear helical structures by X-ray crystallography.

Introduction

Ligand designs that can predispose proximate metal binding sites and organise secondary, peripheral interactions are important for the control of chemical structure and reactivity.[1, 2, 3, 4] In particular, metal-catalysed chemical transformations of small molecules such as O_2, H_2O, CO_2, H_2, and N_2, that are intrinsic to both natural and technologically significant processes, rely upon pre-organised reaction centres that can manage substrate and intermediate binding and efficient electron and proton transfers through coordinative and supramolecular bonding interactions.[2, 5] The development of simple ligand constructs, often inspired by fundamental features of more complex metalloenzymes has led to a plethora of elegantly designed ligands that tailor the metal reaction environment, such as through the generation of deep cavities,[6] second metal binding sites,[4, 7, 8, 9] and/or acid/base or redox appendages,[1, 10, 11] Highly specialised ligands such as picket-fence,[12] crown,[13] Pacman,[7] and Hangman porphyrins,[10] have been developed to introduce axially positioned metal binding sites or acid-base appendages and provide correlation with the proton and electron delivery pathways found in metalloenzymes that carry out these important transformations.[9] Unfortunately, the multi-step synthetic routes towards many of these ligands can be inefficient and time-consuming, so limiting their technological applicability.

We have shown previously that Schiff-base pyrrole macrocycles H_4L that contain two N_4-pyrrole-imine donor sets separated by two *o*-aryl hinges can be prepared in three, high yielding steps without the need for high dilution techniques;[14, 15] Sessler and co-workers prepared the same macrocycles independently.[16] Importantly, these macrocycles fold on metallation to form well-defined Pacman-like cleft microenvironments that are

structurally similar to cofacial diporphyrins. Using these ligands, we have been able to access a myriad of d- and f-block redox chemistry, including catalytic oxygen reduction by cobalt complexes.[14, 17, 18] However, our efforts to prepare mononuclear transition metal complexes to assess the potential of the proximal and vacant N_4 donor set was thwarted by an allosteric preference for bimetallic complex formation. Even so, mononuclear macrocyclic uranyl complexes were prepared, were found to adopt Pacman structures, and show unprecedented oxo group reactivity on manipulation of the vacant N_4-donor compartment.[19] Furthermore, mononuclear tin and binuclear tin/iron and tin/zinc complexes were also accessible; presumably, the axial ligands at the metal inhibit the complexation of the second metal.[20] In order to promote monometallic complex formation while still accessing secondary sphere control through hydrogen bonding or second, disparate metal coordination, we have developed new ditopic Schiff-base pyrrole macrocycles that incorporate N_4- and O_5 or ONO donor sets; one ligand (H_2L^P) and its Co complexes were communicated previously.[21] In this paper, we report on the full synthetic approaches to five variants of these ligands and a variety of complexes of metals across the Periodic Table, and show how the presence of ditopic sites in this compartmental macrocycle predispose its complexes towards interactions with water guest molecules.

Results and Discussion

Macrocycle syntheses and structures

The reactions between 2-nitrophenol and either polyether or nitrogen aryl dichlorides in the presence of excess potassium carbonate in DMF at 120 °C resulted in the formation of the respective acyclic dinitro compounds (Scheme 1). The reduction of these latter compounds with H_2 in the presence of catalytic amounts of Pd/C resulted in the formation of the corresponding amines in moderate overall yield after workup (*ca*. 45 %). The ^{1}H NMR spectra of the acyclic diamines showed the appearance of a resonance corresponding to NH_2 group at *ca*. 3.9 ppm, with the IR spectra showing the disappearance of the NO_2 absorbances at around 1610 and 1340 cm^{-1} and the appearance of the NH stretch at approximately 3400 cm^{-1}. The [1+1] Schiff-base condensation reactions between the acyclic diamines **1** and the straightforwardly-synthesised dipyrromethane dialdehydes **2** were achieved efficiently in the presence of the Lewis acid $BF_3{\cdot}OEt_2$, forming the macrocycles H_2L^P, H_2Lf^P, H_2L^{NMe}, H_2L^{NMes}, and H_2Lf^{NMe} after neutralisation of the acid salt with a solution of NH_3 in MeOH. Due to more straightforward isolation procedures, the use of the fluorenyl-substituted dipyrromethane resulted in higher overall yields (65 % *cf.* 40-57 % for Et-substituted versions). This synthetic route contrasts to that previously reported for the symmetrical compartmental ligands H_4L,[15, 22] as cyclisation reactions attempted using Brønsted acid catalysts such as CF_3COOH or p-$HOSO_2C_6H_4Me$ resulted in unidentifiable mixtures by ^{1}H NMR spectroscopy.

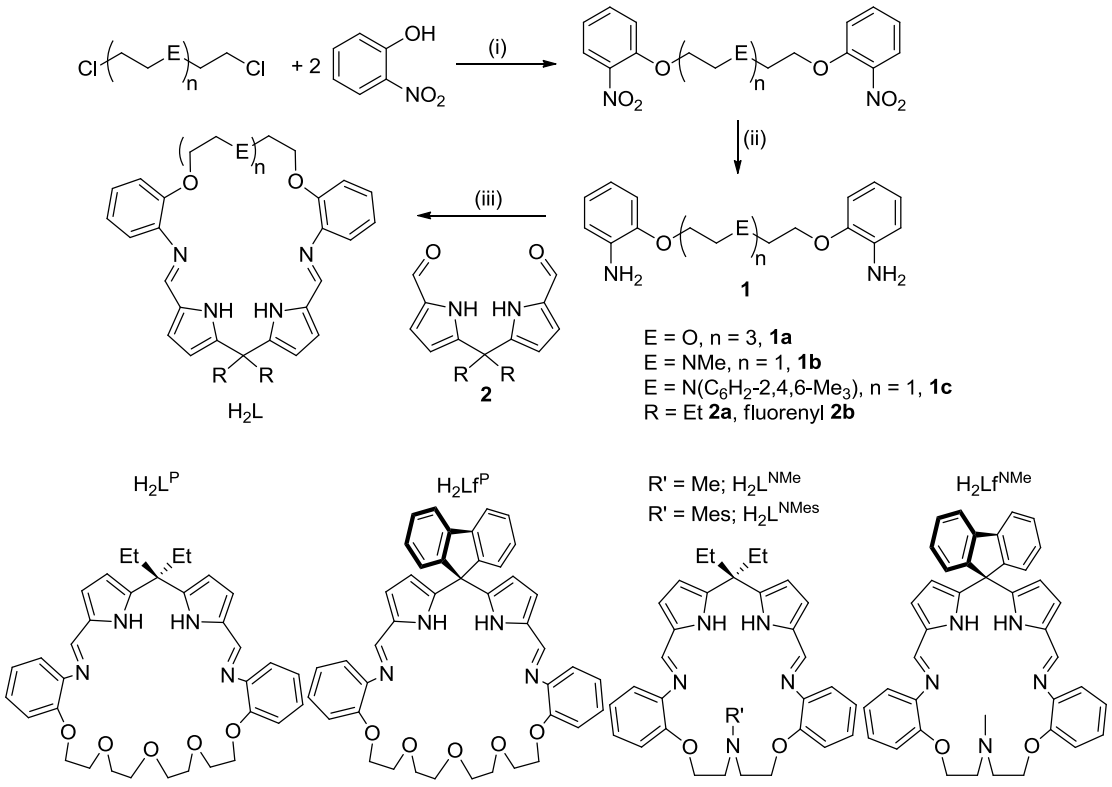

Scheme 1. Synthetic approaches to heteroditopic Schiff-base-pyrrole macrocycles that incorporate either an O_5 or ONO donor compartment. Reagents and conditions: (i) K_2CO_3, DMF, 120 ^oC; (ii) H_2, 10% Pd/C, EtOH; (iii) (a) BF_3OEt_2, EtOH, (b) 7M NH_3 (in MeOH), CH_2Cl_2.

The formation of the macrocycles is supported by ^1H NMR spectroscopy and are exemplified for H_2L^P and H_2L^{NMe} with a resonance at 8.03 (H_2L^{NMe}) or 8.29 ppm (H_2L^P) attributed to the imine N=C(H) proton. A further resonance at 8.69 (H_2L^{NMe}) and 9.13 ppm (H_2L^P) corresponds to the pyrrolic NH with aromatic C-H resonances at 7.00, 6.88, 6.67 and 6.82 ppm (H_2L^{NMe}) and 7.11, 7.50, 6.97 and 6.91 ppm (H_2L^P) and doublets at 6.51 and 6.19 ppm (H_2L^{NMe}) and 6.64 and 6.23 ppm (H_2L^P) indicative of the pyrrolic C-Hs; these assignments were supported by 2D NMR spectroscopy. The single quartet and triplet resonances seen at 1.99 and 0.69 ppm (H_2L^{NMe}) and 2.12 and 0.80 ppm (H_2L^P) for the *meso*-ethyl groups infer flexibility of the structures in solution, which is corroborated by the simplicity of the ether/amine backbones protons, appearing at 4.00 and 2.86 ppm (H_2L^{NMe}) and 4.14, 3.83, 3.66 and 3.48 ppm (H_2L^P). A singlet resonance at 2.37 ppm is attributed to the N-CH_3 protons of the H_2L^{NMe} macrocycle. The ^1H NMR spectra of these macrocycles also showed some broad resonances that are closely related to those of the major product, and are suggestive of higher order cyclisation. The EI mass spectra of H_2L^{NMe} and H_2L^P corroborates the formation of a small quantity of [2+2] cyclised products, with low intensity, high mass peaks seen at 1046 and 1019 (H_2L^{NMe}) and 1198 and 1169 (H_2L^P) amu along with the expected molecular ion peaks at 523 (H_2L^{NMe}) and 598 amu (H_2L^P). In contrast however, no peaks consistent with the [2+2] products are seen in the fluorenyl-substituted

analogues H_2Lf^P and H_2Lf^{NMe} in the EIMS. Attempts to purify these materials by column chromatography (silica or alumina) resulted in complete decomposition of the macrocycle. Unlike the symmetrical macrocycle H_4L, H_2L^P and H_2L^{NMe} are mildly water sensitive with ^1H NMR spectra showing the appearance of an aldehyde resonance at *ca.* 9.2 ppm when a sample was left exposed to air.

A crystal of H_2Lf^{NMe} suitable for single crystal X-ray diffraction was grown by hexane diffusion into a THF solution and the solid state structure was determined (Figure 1). Two crystallographically independent molecules were found in the asymmetric unit, and, due to their similarity, only one will be discussed. In the solid state, the macrocycle adopts a shallow-bowl conformation with the *meso*-fluorenyl group twisted out of the macrocyclic plane (N_4-plane – fluorenyl angle 69.36 °). A water molecule is found hydrogen bonded to one half of the macrocycle, with the macrocycle displaying both hydrogen bond donor and acceptor properties through five different donor/acceptor groups present (O301-donor distances: -N101 2.914, -O102 3.046, -N105 2.863 Å, O301-acceptor distances: -N102 2.847 and -C108 3.610 Å); the hydrogen atoms for O301 were not located in the difference Fourier map. Similar interactions between the pyrrole NH donors and imine N acceptors in H_4L and solvent of crystallisation were seen previously,[22, 23] and an analogous weak interaction between the fluorenyl substituent (C108) and the metal-bound hydroxide was seen in a related binuclear cobalt complex of the symmetric macrocycle ($C_{fluorenyl}$-O 3.386 Å) and could play a role in any future catalytic chemistry.[17] The second pyrrolic nitrogen (N103) is not involved in any further bonding. All the bond distances observed are similar to those of related symmetric macrocycles employing either the *meso*-fluorenyl or other *meso*-substituents, such as the imine (C101–N101 1.284(2) Å) compared to 1.280(8)–1.289(3) Å and C_{arene}-N101-C101 bond angle of 120.25(16) °, compared to 119.7(5)–121.0(3) ° for related symmetric macrocycles.

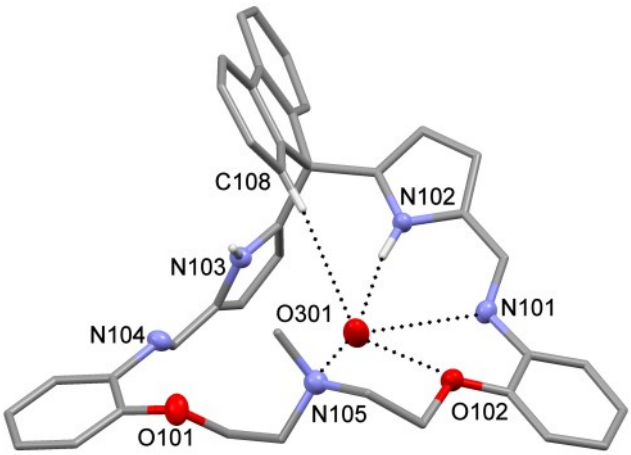

Figure 1. X-ray crystal structure of the heteroditopic Schiff base pyrrole macrocycle H_2L^{NMe}. For clarity, only one of two molecules in the asymmetric unit is shown, and hydrogen atoms except those involved in hydrogen-bonding interactions are omitted (displacement ellipsoids are drawn at 50% probability).

Metal complexes of heteroditopic macrocycles

Potassium and magnesium complexes

In order to facilitate salt elimination reactions, the red di-potassium salts $K_2(L^P)$, $K_2(L^{NMe})$, $K_2(Lf^P)$, $K_2(Lf^{NMe})$, and the yellow magnesium salts $Mg(L^P)$ $Mg(L^{NMe})$, $Mg(Lf^P)$, and $Mg(Lf^{NMe})$ were prepared by reaction of THF solutions of the protonated macrocycles with KH or $Mg(Bu^n)_2$, respectively (Scheme 2). The ^1H NMR spectrum (double solvent suppression H_8-THF/C_6D_6 capillary) of the potassium salt $K_2(L^{NMe})$ showed the absence of the NH resonance of the free macrocycle (*ca.* 9.5 ppm) and a single imine resonance at *ca.* 8.3 ppm. The low frequency region of the spectrum displayed only one *meso*-ethyl environment at 1.10 ppm with resonances for the *meso*-ethyl-CH_2 and ether/amine backbone lost beneath the suppressed THF resonances. The $^{13}C\{^1H\}$ NMR spectrum also shows one ethyl environment with Et-CH_2 and Et-CH_3 resonances at 30.98 and 9.65 ppm (L^{NMe}) indicating that the geometry of $K_2(L^{NMe})$ is fluxional in solution; the NMR data for $K_2(L^P)$ are similar. This contrasts to the potassium salt of a symmetric version of the ligand in which two environments for *endo*- and *exo-meso* substituents were observed.[24] The successful syntheses of $K_2(L^{P/NMe})$ was also confirmed by microanalytical data and by EI mass spectroscopy, the latter showing parent peaks at 599 ($K_2(L^{NMe})$) and 674 amu ($K_2(L^P)$). Furthermore, the IR spectra show the disappearance of the NH stretch at *ca.* 3200 cm^{-1} and a shift in the imine absorbance from *ca.* 1620 to 1560 cm^{-1}.

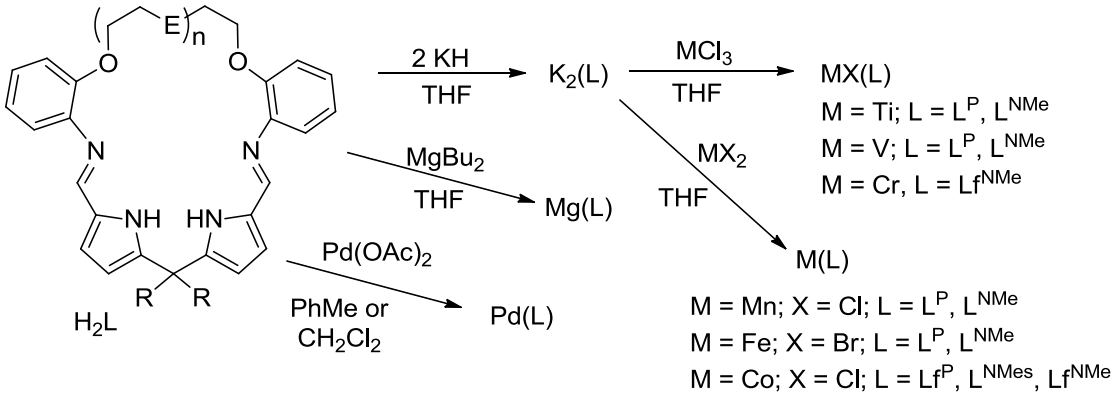

Scheme 2. Synthetic routes to metal complexes of heteroditopic macrocycles H_2L.

Crystals of $K_2(L^P)$ suitable for single crystal X-ray diffraction were grown by slow diffusion of hexane into a H_8-THF/C_6D_6 solution (Figure 2). In the solid state, K_2L^P adopts a helical structural motif with interactions between each potassium cation and the π-system of the arene-backbone units of adjacent molecules resulting in an infinite chain extended structure. Each potassium atom is seven-coordinate, bound in a κ^1 binding mode to one pyrrolic and one imine nitrogen, three ethereal oxygens (O3 bridging between the two potassium atoms

K1 and K2), in a η^5-fashion to a pyrrolic π-system (e.g. K1 to N3 pyrrole) and in a η^2-mode to the arene-backbone π-system; however, some of these interactions are very weak. The K-N_{py} distances of 2.683(2)–2.715(2) Å are shorter than those of the potassium salt of the symmetric ligand K_4L (2.811(2)–2.915(3) Å)[24] and the one reported porphyrin structure (2.740(7)–2.794(6) Å).[25] These distances are more comparable to those seen in the structures of di-potassium diimine-dipyrromethane chelates previously reported by us (2.676(3)–2.976(3) Å),[26] and the adoption of this structural mode can be attributed to the increased flexibility of the (L^P) ligand compared to the Pacman macrocycles L. The K-η^5 centroid distances of 3.276 (K2) and 3.460 (K1) Å are, however, very long. In both $K_4(L)$ and in the above imine-pyrrole salts the K-η^5-centroid distances of 2.962 and 2.903 Å, respectively, are appreciably shorter, with the longest reported K-η^5-pyrrole distance of 3.309 Å for a niobium complex of a tripodal ligand.[27] The majority of K-O distances (2.750(2)–3.134(3) Å) are of a standard length though μ_2-O3 is only weakly bonding to K1 (3.540 Å) compared to K2 (2.908(2) Å), which is compensated by the relatively short K1-O4 distance of 2.625(2) Å.[28] Intermolecular interactions between potassium and the arene-backbones (K-centroid-C16'-C21', 3.386 and 3.590 Å) are also weak, with reported K-η^6-arene-centroid distances ranging from ca. 2.752 to 3.406 Å.[29] Attempted bulk isolation of the potassium salts $K_2(L^P)$ and $K_2(L^{NMe})$ by either precipitation with hexane or by removal of the THF solvent under vacuum proved problematic, with some decomposition to the free ligand $H_2(L^{P/NMe})$ observed in the ^{1}H NMR spectrum. Therefore, $K_2(L^{P/NMe})$ was synthesised *in-situ* in any attempted metallations by salt elimination routes.

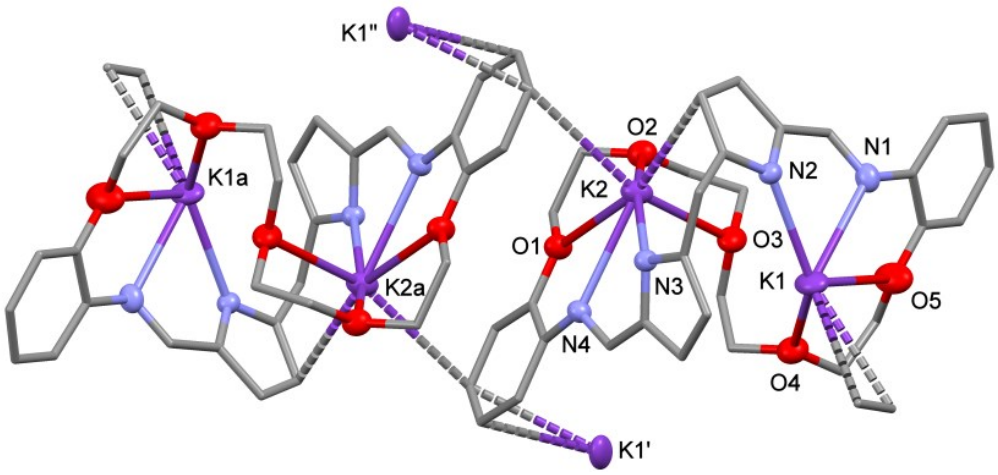

Figure 2. X-ray crystal structure of $K_2(L^P)$. For clarity, hydrogen atoms and solvent of crystallisation are omitted (displacement ellipsoids are drawn at 50% probability)

In a similar manner, the magnesium complexes $Mg(L^P)$, $Mg(L^{NMe})$, $Mg(Lf^P)$, and $Mg(Lf^{NMe})$ were prepared as bright yellow solids (dichroic in solution) in high yields by the addition of a heptane solution of dibutyl-magnesium to each macrocycle. The ^{1}H NMR spectra of these complexes are consistent with the adoption of Pacman geometries in solution as two *meso*-ethyl resonances and the desymmetrisation of the ether/amine

backbone was seen. Furthermore, the ^{1}H NMR spectra show the absence of the NH resonance at *ca.* 9.2 ppm, the loss of which is also seen in the IR spectra along with a shifting of the imine absorbance from *ca.* 1620 to 1565 cm^{-1}. The ^{1}H NMR spectrum of Mg(L^{P}) displays two triplets at 1.16 and 0.89 ppm and two quartets at 2.38 and 2.12 ppm, corresponding to two ethyl environments, and seven separate multiplet resonances between 3.75 and 2.90 ppm, six integrating to two protons and one to four protons, assigned to the desymmetrised polyether backbone. The two *meso*-ethyl environments are also observed in the ^{13}C{^{1}H} NMR spectrum at 11.48 and 10.52 ppm (CH_3) and 41.47 and 34.33 ppm (CH_2) with only four ether-CH_2 resonances at 71.04, 70.72, 70.63 and 70.24 ppm indicating only the protons of the ether backbone are desymmetrised. All of these assignments were confirmed by COSY and ^{1}H-^{13}C HSQC NMR analysis. The EI mass spectrum of Mg(L^{P}) shows a molecular ion peak at 621 amu and elemental analysis supports its formulation.

Palladium complexes

Palladium complexes of the heteroditopic macrocycles were targeted due to the propensity of Pd^{II} to adopt square planar geometries in the pyrrole-imine N_4 donor set. Accordingly, reactions between $Pd(OAc)_2$ and H_2L^{P}, H_2L^{NMe}, H_2L^{NMes}, H_2Lf^{P}, and H_2Lf^{NMe} in toluene or CH_2Cl_2 in the presence of NEt_3 resulted in the formation of the palladium complexes Pd(L^{P}), Pd(L^{NMe}), Pd(L^{NMes}), Pd(Lf^{P}), and Pd(Lf^{NMe}) in moderate to good yields as yellow solids. Characterising data are exemplified for Pd(L^{NMe}). In the ^{1}H NMR spectrum, the NH resonance at 8.69 ppm in the free macrocycle is absent and the imine resonance has shifted from 8.03 to 7.52 ppm, a characteristic also seen in the bimetallic complex Pd_2(L).[15, 22] While the flexibility of the macrocycle H_2L^{NMe} in solution causes resonances for the *meso*-ethyl groups and the backbone CH_2 groups to be equivalent, it is clear from analysis of the low frequency region of the ^{1}H NMR spectrum that a more rigid structure consistent with a Pacman-clefted structure is formed. Two quartets at 2.16 and 2.07 ppm and two triplets at 0.56 and 0.53 ppm correspond to two *meso*-ethyl groups in different environments. Furthermore, the backbone resonances are split into four separate resonances at 4.06, 3.60, 3.02 and 2.85 ppm, each integrating to two protons. This desymmetrisation is mirrored in the ^{13}C{^{1}H} NMR spectrum which displays resonances for two distinctive ethyl groups (CH_3 at 10.0 and 9.7 ppm, CH_2 at 46.5 and 37.0 ppm) and two resonances corresponding to the backbone carbons at 68.0 and 55.2 ppm. The IR spectrum shows the absence of an NH stretch at *ca.* 3200 cm^{-1} and a shift in the imine absorption from 1620 to 1560 cm^{-1}, again as observed for the binucleating H_4L ligands upon metallation. The EI mass spectrum displays the molecular ion at 627 amu, and microanalysis supports the expected formulations. Once synthesised, and unlike the free macrocycles, the palladium complexes are stable to both water and air, with their ^{1}H NMR spectra unchanged after weeks exposed to air.

Crystals of Pd(L^{NMe}), Pd(L^{NMes}), and Pd(Lf^{NMe}) suitable for X- ray crystallography were grown and their solid state structures determined (Figure 3). All three complexes adopt Pacman cleft conformations in the solid state

which correlate well to their structures in solution. In the solid state structure of Pd(L^{NMe}) the asymmetric unit contains two molecules in slightly different conformations, and, due to the similarity of the environment around the palladium, only one of the structures will be discussed. The geometry at the palladium is very similar to that seen in the symmetrically-disposed binuclear palladium complexes $Pd_2(L)$.[15, 22] Palladium-imine (2.093(2)–2.096(2) Å) and palladium-pyrrole bond lengths (1.945(2)–1.943(2) Å) are comparable to $Pd_2(L)$ complexes (Pd-N_{im} 2.043(7)–2.096(2) Å, Pd-N_{py} 1.928(4)–1.947(4) Å). Bond angles are also comparable, with N_{im}-Pd-N_{im} (112.91(9) °) and N_{im}-Pd-N_{py} (79.96(9)–80.07(9) °) similar to those of $Pd_2(L)$ N_{im}-Pd-N_{im} (109.9(4)–119.7(5) °), N_{im}-Pd-N_{py} (79.7(3)–81.4(4) °). The N_{py}-Pd-N_{py} angle of (86.98(9) °) is marginally more acute than in the Pd_2L complexes N_{py}-Pd-N_{py} (88.01(17)–88.8(3) °), though similar to that of other bimetallic complexes of L (N_{py}-M-N_{py} (84.80(13)–88.8(3) °).[22] The conformation of the two Pd(L^{NMe}) molecules in the asymmetric unit differ due to the orientation of the N-Me group, with one positioned towards, and the other away from, the palladium centre. The flipping and twisting of the ether/amine backbone causes the nitrogen of this backbone to move by almost 1.1 Å relative to Pd1, a feature which could be important should groups other than the relatively unencumbered aminomethyl group be employed for proton delivery. These two structures could be considered as an "open mouth" and a "closed mouth" Pacman. Furthermore, the increased flexibility of the ether/amine backbone compared to the more rigid symmetric version allows the aryl hinges to twist to a much greater angle (23.41–46.75 °) compared to reported structures of the type $M_2(L)$ (0.3–32.2 °)[22, 30]

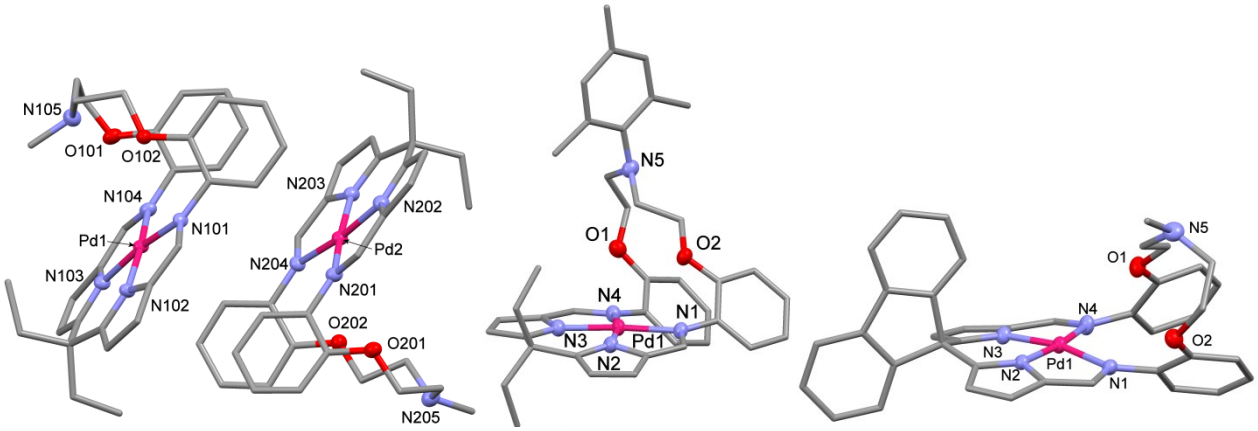

Figure 3. X-ray structures of the Pd complexes Pd(L^{NMe}) (left), Pd(L^{NMes}) (middle), and Pd(Lf^{NMe}) (right). For clarity, hydrogen atoms and solvent of crystallisation are omitted (displacement ellipsoids are drawn at 50% probability).

In the structure of Pd(L^{NMes}), the bulky mesityl group is desymmetrised, with the mesityl-arene ring almost perpendicular to the N_4-plane at an angle of 84.23 ° and orthogonal to the O1-N5-O2 linker. This orientation correlates with that seen in solution; in the ^{1}H NMR spectrum, three distinct resonances for the mesityl methyl

protons are seen at 2.23, 2.20, and 2.10 ppm. There is possibly a weak π- π interaction between this mesityl group and the arene-hinge of an adjacent complex with the distance between ring-centroids being 4.512 Å. With regards to the solution-state structure, aryl-amines are known to have restricted rotation due to electron donation of the nitrogen lone pair into the π system of the arene; however, this would cause the mesityl group to be roughly parallel with the N_4-plane. As such, it is likely that the restricted rotation is caused by a combination of the steric demand of the *o*-methyl substituents and the rigidity of the Pacman geometry. In the extended structure of Pd(L^{NMes}) a molecule of hexane is found sandwiched between two PdN_4 planes oriented in a parallel fashion, with C-arene distances between 3.97 and 4.57 Å.

The solid state structure of Pd(Lf^{NMe}) is similar to the other Pd complexes in which the palladium sits in the N_4-plane (Pd···N_4 0.076 Å) in a distorted square planar environment (Σ Pd angles = 359.82 °). The sp^3-hybridised *meso*-carbon allows for lateral displacement of the *meso* substituents, and in this case the fluorenyl group is oriented towards the cleft at an angle of 23.50 ° relative to the N_4-plane.

Titanium, vanadium, and chromium complexes

Salt elimination reactions between *in-situ* generated $K_2(L^{P/NMe})$ and $TiCl_3(THF)_3$ resulted in the formation of $TiCl(L^P)$ and $TiCl(L^{NMe})$ in moderate yields (*ca.* 50 %). The Ti complexes are highly paramagnetic and silent in their ^{1}H NMR spectra, though their formulations are supported by elemental analysis. Parent ion peaks were seen in the EI mass spectra at 604 (L^{NMe}) and 679 amu (L^P). Once again, the IR spectra show the absence of the NH stretch at *ca.* 3200 cm^{-1} and the shifting of the imine absorbance from 1620 to 1580 cm^{-1}. Crystals of $TiCl(L^P)$ suitable for X-ray diffraction studies were grown by the slow diffusion of hexanes into a THF solution (Figure 4). Unusually, the titanium centre adopts a distorted, seven-coordinate, pentagonal-bipyramidal geometry with four nitrogen donors (two pyrrolic, two imino) and one ethereal oxygen in the equatorial plane and a chloride and ethereal oxygen occupying the axial sites. This structure is the only one of all these complexes in which the pendant O_5 or ONO donor pocket binds directly to the metal centre bound in the pyrrole-imine N_4 donor plane. The highly oxophilic nature of titanium has resulted in a large distortion of the ligand, causing one of the arene backbone units to twist heavily to accommodate the coordination of O1 and O2 to the titanium; however, the overall Pacman geometry is maintained. The two Ti-N_{im} bond lengths (Ti1-N4 2.195(2) and Ti1-N1 2.285(2) Å) differ from each other by 0.09 Å which is likely the result of steric interactions and are longer than those of Ti(III)-salen complexes (2.106(4)–2.139(9)),[31] This is accompanied by a very obtuse N_{im}-Ti-N_{im} bond angle of 134.41(10) ° that is attributed to the heavily-twisted arene backbone. The Ti-N_{py} distances (2.117(3)/2.150(3) Å) are comparable to the few known structures of Ti(III)-pyrrole complexes (2.096(4)–2.136(2) Å).[32] The ether backbone forms an equatorial interaction with the titanium, with a Ti1-O1 distance of 2.382(2) Å, and a stronger axial bond with a Ti1-O2 bond length of 2.219(2) Å. These bond lengths are comparable to previously reported Ti(III)-O ether bonds (2.109(4)–

2.232(2) Å).[33] The chloride is bound *exo* to the cleft at a Ti1-Cl1 distance of 2.3843(11) Å, which is a standard nitrogen/oxygen-bound-Ti(III)-Cl distance (2.324(2)–2.415(2) Å).[34] There is also a weak hydrogen-bonding interaction between the chloride and one of the aryl backbones of an adjacent molecule, with a C34···Cl1 distance of 3.616 Å.

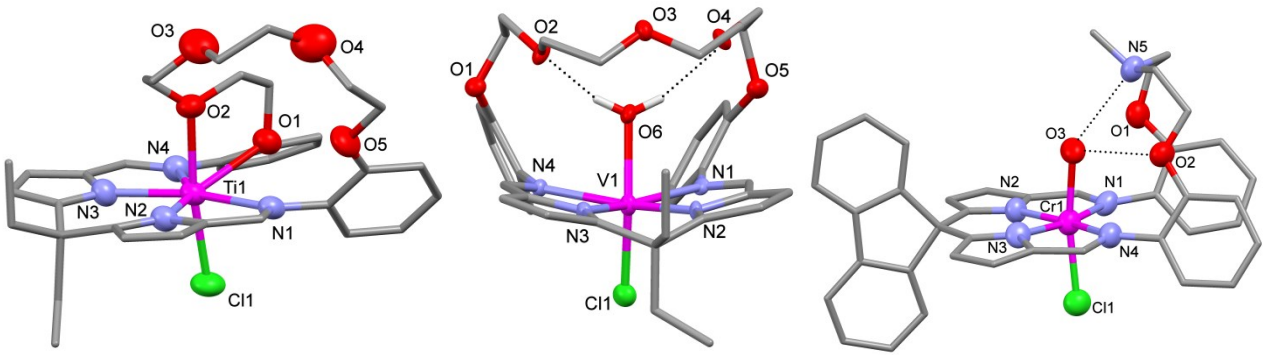

Figure 4. X-ray structures of TiCl(L^P), V(OH_2)Cl(L^P), and Cr(OH_2)Cl(Lf^{NMe}). For clarity, hydrogen atoms except those involved in hydrogen-bonding interactions and solvent of crystallisation are omitted (displacement ellipsoids are drawn at 50% probability).

Addition of *in-situ* prepared $K_2(L^{P/NMe})$ to a stirring suspension of $VCl_3(THF)_3$ caused an immediate change in colour from pink to deep red, and resulted in the formation of the complexes (VCl)(L^P) and (VCl)(L^{NMe}) in moderate yield (*ca.* 60 %) as red solids after workup (Scheme 2). As with the Ti(III) complexes, the products are highly paramagnetic and are silent in their ^{1}H NMR spectra. The EI mass spectra display low intensity parent ions at 683 for VCl(L^P) and 607 amu VCl(L^{NMe}), with higher intensity peaks showing the loss of the chloride ligand. Elemental analyses for both complexes support their formulation. The IR spectra show the disappearance of the NH stretch at *ca.* 3200 cm^{-1} as well as the expected shifting of the imine absorbance from *ca.* 1620 to 1560 cm^{-1}. Crystals of VCl(L^P) suitable for X-ray crystallography were grown by slow diffusion of hexanes into a THF solution (Figure 4). It is clear from the structure that the complex has scavenged water present in the glove-box atmosphere at < 1ppm. The Pacman-shaped complex contains a V(III) cation bound in a distorted octahedral environment with a hydrogen-bonded water molecule accommodated within the cleft. The vanadium sits slightly outside of the cleft, 0.186 Å below the N_4-plane, bound by two imine and two pyrrolic nitrogens. The vanadium-N_{im} distances of 2.195(3) and 2.198(3) Å are slightly longer than for a

similar complex of the symmetric ligand (*ca.* 2.14 Å)[24] and are fairly long compared to V(III)-salen complexes (2.042(3)– 2.166(3) Å)[35] though are within the ranges for other V(III)-N_{im} complexes (2.003(8)–2.242(3) Å).[36] There are a few examples of structurally-characterised vanadium(III) pyrrolide complexes, with V-N_{py} distances of ranging from 1.952(3) to 2.119(6) Å,[37] similar to those reported here (1.998(3)–2.023(3) Å). The axially-bound chloride resides *exo* to the cleft, with a bond distance of 2.2390(12) Å, shorter than that in the binuclear analogue (*ca.* 2.32 Å) as well as being short compared to V(III)-salen complexes (2.286(4)–2.352(2) Å).[38] The arene backbone units have splayed open, so forming an angle of 55.91°, that is similar to that seen in binuclear vanadium,[24] uranyl[39] and alkyl-tin[20] complexes of the symmetric ligand L. The chloride is slightly bent towards the arenes with a O6-V1-Cl1 angle of 158.58(8)°, leading to a weak hydrogen-bonding interaction between the chloride and backbone arene groups (Cl-C_{arene} *ca.* 3.7 Å). Significantly, an axially-bound water molecule resides within the cleft. The V1-O6 bond distance of 2.111(3) Å is characteristic of a V(III)-OH_2 bond and not an oxidized V(IV)=O bond. Examples of V(III)-water interactions are relatively rare, with the V1-O6 bond distance being only slightly longer than reported V(III)-OH_2 distances (1.970(3)–2.108(2) Å),[40] whereas bond lengths of octahedral V(IV)=O are considerably shorter and are in the region of 1.578(2)–1.631(3) Å.[41] The water molecule is further stabilised by hydrogen bonding to the polyether oxygens O2 and O4 distances of 2.753 and 2.804 Å from O6 and shows that the structural motif is ideally oriented to stabilise guest molecules through both primary and secondary sphere bonding interactions.

The reaction between $CrCl_3(THF)_3$ and K_2Lf^{NMe} resulted in the formation of the red Cr(III) complex $CrCl(L^{NMe})$ in good yield. The complex is paramagnetic and silent in the ^{1}H NMR spectrum, although formation of the desired product was indicated by elemental analysis. The IR spectra give the characteristic shifts in the imine stretch and the absence of an NH stretch. Crystals of $CrCl(OH_2)(Lf^{NMe})$ suitable for X-ray crystallography were grown by slow diffusion of C_6D_6 into a $CDCl_3$ solution (Figure 4). The complex contains a Cr^{3+} cation bound in a distorted octahedral environment with a molecule of water accommodated within the molecular cleft. As with the above vanadium complex, it is apparent that water has been scavenged during the crystallisation process. The Cr sits in the N_4-plane and is coordinated by two imine and two pyrrolic nitrogens at standard distances. Although the hydrogen atoms on O3 were not located in the difference Fourier map, the Cr1-O3 bond distance of 2.059(5) Å is similar to that of similar Cr(III) porphyrinic and cyclam complexes that have both chloride and water coordinated (range 1.996 – 2.090 Å).[42] The Cr1-Cl1 distance of 2.301(1) Å is also consistent with the presence of a Cr(III) cation. The water molecule O3 is stabilised by hydrogen bonding to O2 (O2···O3 2.806(2) Å) and the pendant nitrogen N5 (N5···O3 2.846(2) Å), again indicating that this heteroditopic Pacman motif is tailored towards the accommodation of small molecules within the cleft through both primary and secondary sphere interactions. This hydrogen-bonding interaction is also indicated by the bending of O3 towards the backbone, resulting in a Cl-Cr1-O3 angle of 171.15 °.

Cobalt complexes

Reaction of *in-situ* generated $K_2(Lf^{P})$ or $K_2(Lf^{NMe})$ with one equivalent of $CoCl_2$ resulted in the formation of the cobalt complexes $Co(Lf^{P})$ or $Co(Lf^{NMe})$ in low yield (*ca*. 20 %) as red solids (Scheme 2). The ^{1}H NMR spectra are paramagnetically shifted and broadened, though the number of resonances and the values of their integrals are consistent with a Pacman geometry in solution. Specifically, $Co(Lf^{P})$ displays 22 resonances between +60 and −37 ppm, including eight which integrate to 1H corresponding to a non-equivalent protons of the fluorenyl group, as well as seven resonances indicating dissimilar ethereal protons (one resonance integrating to 4H is assumed to be two overlapping 2H resonances). Similarly, the ^{1}H NMR spectrum of $Co(Lf^{NMe})$ displays 19 resonances from +45 to −18 ppm, with six resonances integrating to 1H, with two 1H resonances overlapping, eleven resonances integrated to 2H and one 3H resonance. Elemental analysis supports the formulation of $Co(Lf^{NMe})$ and the EI mass spectra show parent ion peaks at 674 for $Co(Lf^{NMe})$ and 749 amu for $Co(Lf^{P})$. The IR spectra also show the absence of the NH stretch at 3200 cm^{-1} and the standard shifting of the imine absorption from 1620 to 1560 cm^{-1}. Exposure of THF solutions of $Co(Lf^{P})$ and $Co(Lf^{NMe})$ to air results in wholly diamagnetic ^{1}H NMR spectra that are indicative of the formation of Co(III) complexes. Although the clean isolation of the highly insoluble $Co(OH_2)(OH)(Lf^{NMe})$ was not successful, the new Co(III) aqua-hydroxy complex $Co(OH_2)(OH)(Lf^{P})$ was characterised. The ^{1}H NMR spectrum of $Co(OH_2)(OH)(Lf^{P})$ displays a series of multiplets, some of which overlap, in the arene region 7.78–6.18ppm, which indicates non-equivalence of the protons of the fluorenyl group, and overlapping multiplets from 3.48–2.72 ppm indicative of dissimilar backbone ethereal protons. This ligand desymmetrisation is also mirrored in the $^{13}C\{^1H\}$ NMR spectrum with 15 CH and 8 quaternary carbon resonances between 163 and 106 ppm and is also indicative of a Pacman geometry in solution. Microanalysis supports the formulation and the IR spectrum shows absorptions at 3409 and 3232 cm^{-1} that are assigned to OH stretches.

Crystals of $Co(OH_2)(OH)(Lf^{P})$ suitable for X-ray diffraction were grown from an air-saturated toluene solution of $Co(Lf^{P})$ (Figure 5). Unfortunately, due to poor quality of the data leading to a high R factor of 12.9 %, an in-depth discussion of the structure is not possible. The complex displays a Pacman structure in which Co1 adopts a distorted octahedral geometry. Comparison to the crystal structure of the related complex $Co(OH_2)(OH)(L^{P})$ suggests that the axial ligands are water and hydroxide, with the water O6 within the cleft and the hydroxide O7 outside the cleft.[21] Due to the presence of the fluorenyl substituent and its weak interaction as a hydrogen bond donor to the in-cleft water molecule, the arene hinges and polyether backbone are heavily twisted, with only O5 hydrogen bonded to the water within the cleft. This allows a linear chain of hydrogen bonds to build up between adjacent molecules. In particular, the exogenous hydroxide is hydrogen bonded to a second water molecule (O7···O100 2.475 Å), which is in turn hydrogen bonded to the endogenous water of an adjacent Pacman complex (O100···O6’ 2.677 Å), so creating a Co-Pacman "water wire" and not a six-membered hydrogen-bonded wheel as seen in the structure of $Co(OH_2)(OH)(L^{P})$.[21]

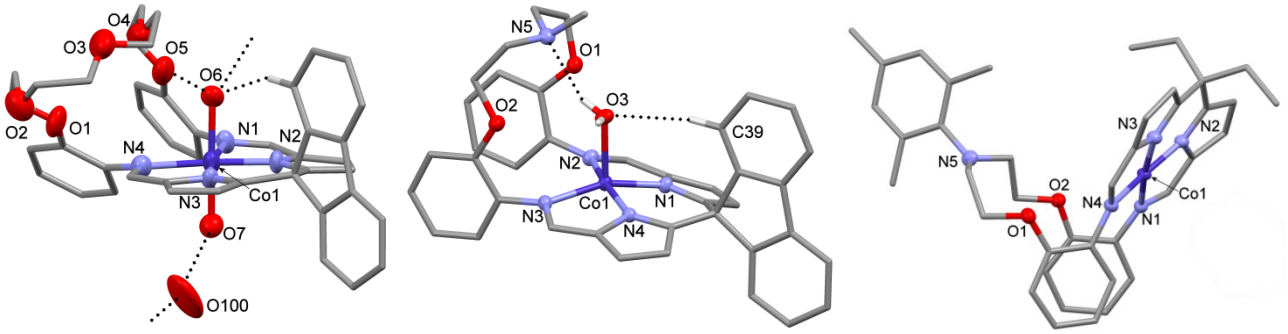

Figure 5. X-ray structures of $Co(OH_2)(OH)(Lf^{P}).(H_2O)$, $Co(OH_2)(Lf^{NMe})$, and $Co(L^{NMes})$. For clarity, hydrogen atoms and solvent of crystallisation are omitted (displacement ellipsoids are drawn at 50% probability).

The solid state structure of $Co(Lf^{NMe})$ was determined and while the Co(II) oxidation state was retained, a molecule of water was again scavenged and located within the Pacman cleft. In $Co(OH_2)(Lf^{NMe})$, the Co adopts a distorted square pyramidal geometry with pyrrole (N1/N4) and imine N2/N3) nitrogen donor atoms making up the basal plane and the oxygen donor (O3) apical. The Co sits above the N_4 donor set by 0.21 Å, with a Co1-O3 distance of 2.156(1) Å in the range expected for similar Co(II) aquo phthalocyanines (2.215 Å)[43] and amine macrocycles (2.171 and 2.282 Å).[44] The hydrogen atoms on O3 were located from the difference Fourier map and are oriented towards the amine nitrogen N5 (O3…N5 2.862 Å) and a pyrrole group of an adjacent molecule (O3…C3' 3.442 Å). Short interactions are also seen between O3 and the ethereal oxygen atoms O1 (O3…O1 3.173 Å) and O2 (O3…O2 3.125 Å), and the fluorenyl substituent is oriented such that it acts as a hydrogen bond donor to O3 (O3…C39 3.561 Å). As such, the molecule of water sits in a hydrogen bonded cavity made up from the peripheral substituents of the macrocyclic ligand.

The X-ray crystal structure of $Co(L^{NMes})$ was determined, and the structure was found to be similar to its Pd analogue $Pd(L^{NMes})$, with an overall Pacman motif seen and the Co(II) cation residing in a square-planar environment, 0.56 Å above the N_4 donor plane. The Co-N distances (Co1-N_{im} 1.977(2)-1.999(2) Å; Co1-N_{py} 1.862(2)-1.864(2) Å) are similar to those seen in the above complexes and appear invariant to the Co oxidation state, a feature that we have noted previously in the study of dioxygen adducts of binuclear Co Pacman complexes.[17, 45, 46] The bulky mesityl-substituted amine N5 is oriented away from the metal centre, resulting in a Co1-N5 separation of 5.600 Å, with the aryl group orthogonal to the ONO chelate and perpendicular to the N_4 plane (85.16 °). As with $Pd(L^{NMes})$, the desymmetrisation of the mesityl group seen in the solid state is reflected in solution, with five Me resonances for the mesityl and ethyl substituents seen in

the ^{1}H NMR spectrum at 3.68, 0.44, -0.12, -30.16, and -33.01 ppm, and indicating that rotation about the N-C bond of the mesityl amine group is restricted.

Manganese, iron, and cobalt [2+2] macrocyclic complexes

The filtration of *in-situ* generated $K_2(L^P)$ or $K_2(L^{NMe})$ on to a stirred suspension of $FeBr_2(THF)_2$ in THF resulted in a colour change from orange to deep red and the isolation of the iron complexes [Fe(L^P)] or [Fe(L^{NMe})] after work up in good yields. The ^{1}H NMR spectra of these complexes are paramagnetically shifted and broadened, though the number of resonances and their integrals are consistent with Pacman geometries. Parent ion peaks are seen in the EI mass spectra at 577 for Fe(L^{NMe}) and 652 amu for Fe(L^P). In addition, low intensity, higher mass peaks are also seen in the mass spectrum of Fe(L^P) at 1304 and 1277 amu and indicate the presence of a small amount of a higher cyclisation product. The IR spectra show the absence of the NH stretch at *ca.* 3200 cm^{-1} and the imine absorbance shifting to *ca.* 1560 cm^{-1}, from 1620 cm^{-1}. The elemental analysis of Fe(L^{NMe}) supports its formulation. In a similar manner, the salt-elimination reactions of $K_2(L^{P/NMe})$ with $MnCl_2$ resulted in a colour change from red to deep red and the formation of Mn(L^P) or Mn(L^{NMe}). The ^{1}H NMR spectra are featureless between ±100 ppm, and with all crystallisation attempts unsuccessful, the structures of these complexes cannot be deduced. However, elemental analyses support their formulations, and the mass spectra exhibit molecular ions at *m*/z = 577 for Mn(L^{NMe}) and 651 for Mn(L^P). Furthermore, the absence of NH stretch and shift in the imine absorbance to *ca.* 1560 cm^{-1} were again observed. Attempts to grow crystals of Fe($L^{P/NMe}$) and Mn($L^{P/NMe}$) were unsuccessful. However, a small amount of crystalline material corresponding to [2+2] ligand by-products were isolated from THF solutions of Fe(L^P) and Mn(L^P).

As stated earlier, the ^{1}H NMR spectra of the $H_2L^{P/NMe}$ macrocycles showed the presence of small, broad resonances similar to the major resonances, and the mass spectrum indicated the possible formation of small amounts of a [2+2] cyclisation product. The crystals grown from solutions of Fe(L^P) and Mn(L^P) support this observation as they incorporate a new [2+2] macrocycle ($^{2+2}L^P$) and not the expected 1+1 macrocycle, with the extra flexibility of this new macrocycle allowing the formation of helical geometries. The structures are similar, so only the Fe complex will be discussed (Figure 6). The two Fe cations reside in distorted octahedral environment, slightly out of the N_3O plane ($N_3O\cdots$Fe 0.002 and 0.023 Å) made from two pyrrolic (N2/N7) and one imine nitrogen (N8) and an ethereal oxygen (O6). A further imine nitrogen (N1) occupies one axial position with the other a weaker interaction between the metal and the nitrogen of an opposing pyrrole (Fe1-N7 2.530 Å and Fe2-N3 2.565 Å). The Fe-N_{py} distances (2.049(4)–2.178(4) Å) and Fe-N_{im} distances (2.118(4)–2.130(4) Å) are longer than that of other imine-pyrrole chelates (Fe-N_{py} 2.016(2) and 2.021(2) Å, Fe-N_{im} 2.104(2) and 2.107(2) Å)[26, 47] and iron-complexes of the symmetrical macrocycle L (Fe-N_{py} 2.009(7)–2.025(6), Fe-N_{im} 2.096(6)–2.176(4) Å).[30] These distances are, however, within the ranges seen in iron-porphyrin (Fe-N_{py} 1.972(4)–2.261(5))[48] and iron-imine complexes (1.984(2)–2.241(5)).[49] An intramolecular

face-to-edge π-stacking interaction between an arene hinge and a pyrrole unit is also observed for these two complexes (C_{arene}-centroid$_{py}$ 3.361 and 3.336 Å).

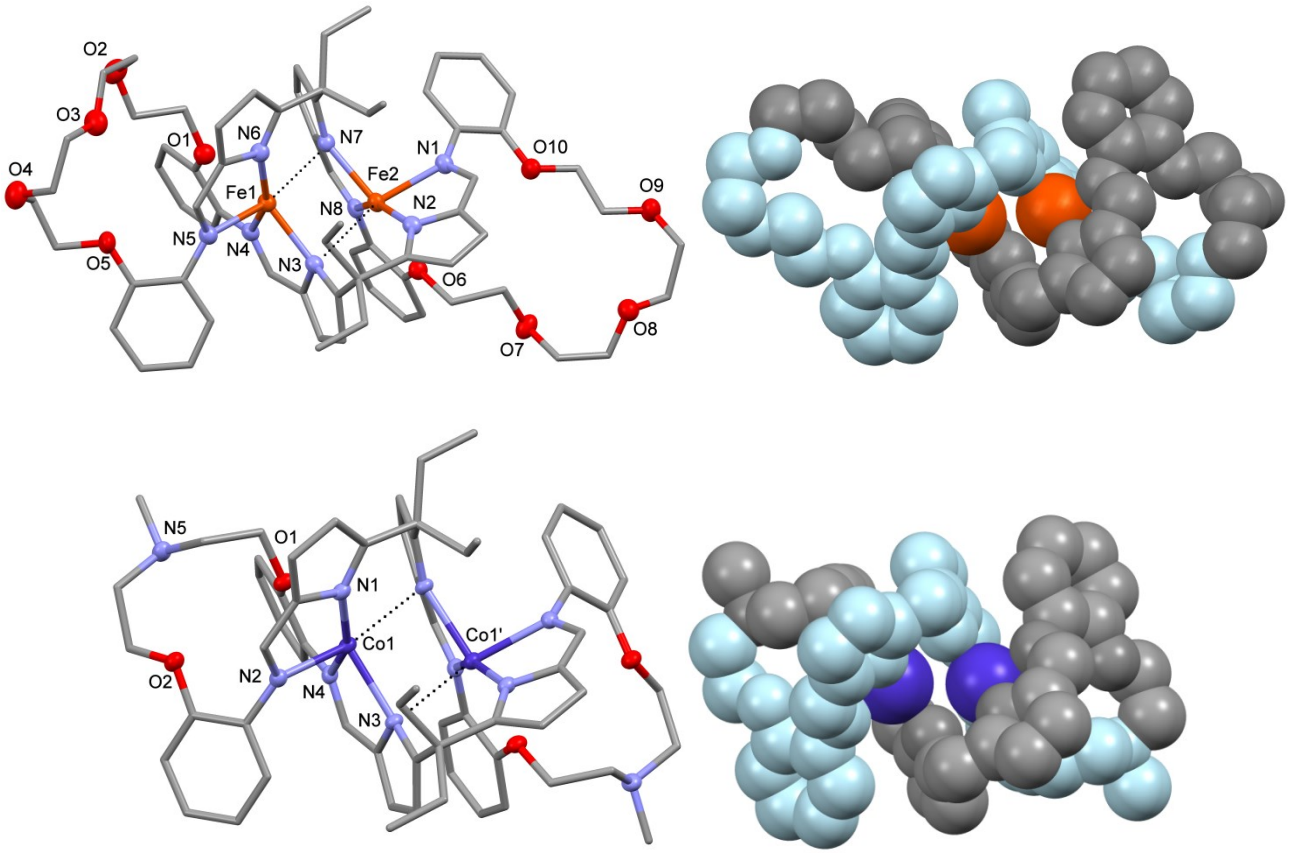

Figure 6. X-ray crystal structures of the [2+2] macrocyclic di-iron complex $Fe_2(^{2+2}L^{P})$ and di-cobalt complex $Co_2(^{2+2}L^{NMe})$ with representative space-filled pictures displaying their helicity. For clarity, all hydrogen atoms, some ethyl substituents, and solvent of crystallisation are omitted (displacement ellipsoids are drawn at 50% probability.

Further to the isolation of the binuclear Fe and Mn complexes of $^{2+2}L^{P}$, a crystal suitable for single crystal X-ray diffraction studies was grown by hexane diffusion into a THF solution of Co(L^{NMe}) and was found to be of the [2+2] cyclised complex $Co_2(^{2+2}L^{NMe})$. As with the above compounds, a helicate structure is observed. The cobalt cation adopts a distorted octahedral geometry, residing 0.024 Å out of the N_3O-equatorial plane. The axial ligands comprise an imine nitrogen as well as a weak pyrrole-N interaction (Co···N_{py} 2.481 Å) similar to the Fe and Mn complexes above. Co-N bond distances (Co-N_{py} 1.997(2) and 2.1642(19) Å and Co-N_{im} 2.072(2) and 2.125(2) Å) are slightly longer than corresponding acyclic imine-pyrrole chelate (Co-N_{py} 1.980(3) and 1.989(3) Å and Co-N_{im} 2.047(3) and 2.055(3) Å) as well as marginally longer than cobalt complexes of the symmetric macrocycle (Co-N_{py} 1.847–1.970(8) Å, N_{im} 1.856(7)–1.984(4) Å)[23, 46] and Co(L^{P})

complexes (Co-N_{py} 1.852(3)–1.8818(18) Å, Co-N_{im} 1.981(1)–2.0335(18) Å). Intermolecular face-to-edge π-stacking interactions between two arene units ($centroid_{arene}$- $centroid_{arene}$ 3.438 Å) are also observed. The imine-pyrrole cores of all the above helicate complexes closely resemble those of helicates of acyclic diimine-dipyrrole chelates synthesised by us.[26, 47, 50] In all cases, the flexibility at the sp^3 hybridised *meso*-carbon facilitates a helical twist and the complexation of two metal centres by both N and O donors. The presence of extended ether/amine groups in the [2+2] ligands enables a distorted octahedral geometry to be attained, rather than the distorted tetrahedral geometry seen previously. This feature results in much shorter M···M separations in the $M_2(^{2+2}L)$ complexes (M···M separations 3.151 (Fe), 3.521 (Mn) and 3.104 Å (Co) Å) compared to those seen previously (Fe: 4.689; Mn: 4.751; and Co: 4.914 Å). [26, 47] The two separate systems are similar in that they both feature a major and minor groove motif, likely due to favourable π-π-stacking between imine/pyrrole and arene groups; further inspection of the structures reveal that racemic mixtures of the helicates are present in the unit cell. In these examples, it is thought that the Mn, Fe, and Co complexes of ^{2+2}L have crystallised preferentially and represent a small fraction of the bulk material. The molecular ion peaks in the mass spectra of bulk Fe(L^P), Mn(L^P) and Co(L^{NMe}) show an isotope pattern consistent with a [1+1] ligand complex with the higher mass peaks of very low intensity. Work on synthesising [2+2] ligands in preference to [1+1] macrocycles or the combination of imine/pyrrole chelates with other flexible linkers is yet to be investigated.

Experimental

All manipulations involving transition metals were carried out using standard Schlenk line or glovebox techniques under an atmosphere of dinitrogen unless stated otherwise. Dry solvents (THF, toluene, CH_2Cl_2, hexane, and MeOH) were purified by passage through Vacuum Atmospheres or MBraun solvent drying towers and stored over activated 4 Å molecular sieves. Deuterated solvents were dried (C_6D_6 and C_5D_5N over potassium, $CDCl_3$ was stirred over activated alumina), trap-to-trap vacuum distilled, and freeze-pump-thaw degassed three times prior to use. Syntheses of $VCl_3(THF)_3$ and $TiCl_3(THF)_3$,[51] 5,5'-diformyldiethyl-2,2'dipyrromethane **2a** and 9,9-Bis(5-formylpyrrole-2-yl)fluorene **2b**,[23] 2,2'-dichloro-N-methyldiethylamine,[52] and tetraethyleneglycolbis(o-nitrophenylether),[53] were carried out as described in the literature. Pyrrole was distilled under reduced pressure prior to use, and all other chemicals were used as purchased.

^1H NMR spectra were recorded at 298 K, unless otherwise stated on Bruker DPX 250, DPX 360, AVA 400, DMX 500, AVA 500, AVA 600 or JEOL ECX 400 spectrometers at operating frequencies of 250.13, 360.13, 399.90, 500.13, 500.12, 599.81 and 391.79 MHz respectively. $^{13}C\{^1H\}$ spectra were recorded on the same spectrometers at operating frequencies of 62.90, 90.55, 100.55, 125.76, 125.76, 150.82 and 98.51 MHz respectively. Two dimensional ^1H-^1H and ^{13}C-^1H correlation experiments were used, when necessary, to confirm ^1H and ^{13}C assignments. All NMR spectra were referenced internally to residual protio solvent (^1H) or

solvent ($^{13}C\{^{1}H\}$) resonances and are reported relative to tetramethylsilane (δ = 0 ppm). Chemical shifts are quoted in δ (ppm) and coupling constants in Hertz. Mass spectra were recorded by Mr Alan Taylor of the mass spectrometry service of Edinburgh University's Department of Chemistry; Electrospray mass spectra were recorded using a Thermo LCQ instrument, EI mass spectra and high resolution mass spectra were recorded using a Mat 900 XP instrument. Elemental analyses were carried out at by Mr Stephen Boyer at London Metropolitan University. IR data were collected on a Jasco FT/IR 410 spectrometer.

X-ray crystallography

Single-crystal X-ray diffraction data were collected on one of five machines: At 100 K using an Oxford Cryosystems low temperature device attached to an Oxford Diffraction SuperNova dual wavelength diffractometer equipped with an Atlas CCD detector and operating mirror monochromated Cu*K*α radiation mode (λ = 1.54184 Å); at 150 K using an Oxford Cryosystems low temperature device attached to an Oxford Diffraction Xcalibur Eos diffractometer equipped with an Eos detector and operating graphite monochromated Mo*K*α radiation (λ = 0.71073Å); at 150 K on a Bruker SMART APEX diffractometer equipped with a CCD area detector using graphite monochromated Mo*Kα* radiation (λ = 0.71073 Å); graphite monochromated Mo*Kα* radiation (λ = 0.71073 Å) at 150 K on a Rigaku MM007 diffractometer equipped with a high brilliance Saturn 70 CCD detector; at 123 K using a Rigaku Mercury CCD system equipped with a Rigaku GNNP low-temperature device with graphite monochromated Mo*Kα* radiation (λ = 0.71073 Å).

The structures were solved using the WINGX suite of programs by direct methods and refined using full-matrix least square refinement on $|F^2|$ using SHELXL-97.[54] Unless otherwise stated, all non-hydrogen atoms were refined with anisotropic displacement parameters while hydrogen atoms were placed at calculated positions and included as part of a riding model. When stated, if modelling of disordered solvent was unsuccessful the SQUEEZE routine of PLATON was used.[55]

Macrocycle syntheses

All of the new, heteroditopic macrocycles were prepared in a manner similar to that described below for H_2L^P using degassed, but not dried solvents unless stated otherwise.

H_2L^P: Under a nitrogen flush, neat BF_3OEt_2 (1.4 mL, 11 mmol) was added dropwise to a mixture of diamine **1a** (1.88 g, 5.0 mmol) and dialdehyde **2a** (1.291 g, 5.0 mmol) in absolute EtOH (150 mL), and the mixture was stirred at room temperature for 2 h, during which a red oil formed. The solvent was decanted and the oil washed with EtOH (2 × 20 mL). The residual oil was dissolved in CH_2Cl_2 (70 mL) and treated with 7 M NH_3 in MeOH (1 mL) causing BH_3NH_3 to precipitate. The solids were filtered and the filtrate evaporated to dryness to yield a fluffy orange solid. Dry THF (20 mL) was added, the mixture filtered from any remaining

BF_3NH_3 and the filtrate evaporated to dryness giving H_2L^P as a yellow/orange solid (1.21 g, 2.02 mmol, 40 %). ^{1}H NMR (399.90 MHz, C_6D_6): δ 9.44 (s, 2H, pyrrole NH), 8.24 (s, 2H, imine), 7.03 (dd, *J* = 7.6, 1.6 Hz, 2H, Ar-H), 6.96 (td, *J* = 7.8, 1.7 Hz, 2H, Ar-H), 6.86 (td, *J* = 7.5, 1.3 Hz, 2H, Ar-H), 6.68 (dd, *J* = 8.0, 1.1 Hz, 2H, Ar-H), 6.55 (d, *J* = 3.6 Hz, 2H, pyrrole), 6.05 (d, *J* = 3.7 Hz, 2H, pyrrole), 3.79–3.74 (m, 4H, OCH_2), 3.62–3.57 (m, 4H, OCH_2), 3.53–3.46 (m, 8H, OCH_2), 1.67 (q, *J* = 7.3 Hz, 4H, Et-CH_2), 0.59 (t, *J* = 7.3 Hz, 6H, Et-CH_3); ^{13}C{^{1}H} NMR (100.55 MHz, C_6D_6): δ 152.3 (s, CH), 151.0 (s, CH), 142.9 (s, quaternary), 141.8 (s, quaternary), 131.5 (s, quaternary), 125.7 (s, CH, Ar-H), 121.9 (s, CH, Ar-H), 121.8 (s, CH, Ar-H), 116.2 (s, quaternary), 114.3 (s, CH, pyrrole), 108.0 (s, CH, pyrrole), 71.5 (s, CH_2, OCH_2), 71.0 (s, CH_2, OCH_2), 69.8 (s, CH_2, OCH_2), 69.7 (s, CH_2, OCH_2), 44.3 (s, quaternary), 29.1 (s, CH_2, Et-CH_2), 8.5 (s, CH_3, Et-CH_3); MS(EI): *m/z* = 598.3 (M^+, 12 %), 569.2 ([M^+–Et]$^+$, 100 %); Analysis. Found: C, 70.08; H, 6.94; N, 9.20. $C_{35}H_{42}N_4O_5$ requires: C, 70.21; H, 7.07; N, 9.36 %; IR (nujol, KBr): ν 3244 (N-H), 1617 (C=N), 1496 cm^{-1} (C=C).

H_2L^{NMe}: diamine **1b** (1.75 g, 5.8 mmol), dialdehyde **2a** (1.498 g, 5.8 mmol), $BF_3{\cdot}OEt_2$ (1.6 mL, 12.2 mmol) yield 57% (1.73 g, 3.30 mmol). ^{1}H NMR (250.13 MHz, $CDCl_3$): δ 8.69 (br, s, 2H, pyrrole NH), 8.03 (s, 2H, imine), 7.00 (m, 2H, Ar-H), 6.88 (m, 4H, Ar-H), 6.82 (d, 2H, *J* = 7.9 Hz, Ar-H), 6.51 (d, 2H, *J* = 3.5 Hz, pyrrole), 6.19 (d, *J* = 3.5 Hz, pyrrole), 4.00 (m, 4H, O/N-CH_2), 2.86 (m, 4H, O/N-CH_2), 2.37 (s, 3H, N-CH_3), 1.99 (q, 4H, *J* = 7.4 Hz, Et-CH_2), 0.69 (t, 6H, *J* = 7.5 Hz, Et-CH_3); ^{13}C{^{1}H} NMR (62.90 MHz, $CDCl_3$): δ 150.5 (s, CH, Ar-H), 149.7 (s, quaternary), 141.6 (s, quaternary), 140.7 (s, quaternary), 129.7 (s, quaternary), 124.6 (s, CH, Ar-H), 120.7 (s, CH, Ar-H), 120.0 (s, CH, Ar-H), 115.5 (s, CH, pyrrole), 112.6 (s, CH, Ar-H), 108.2 (s, CH, pyrrole), 67.3 (s, CH_2, O/N-CH_2), 56.1 (s, CH_2, O/N-CH_2), 42.9 (s, quaternary), 41.8 (s, CH_3, N-CH_3), 27.3 (s, CH_2, Et-CH_2), 7.0 (s, CH_3, Et-CH_3); MS(EI): *m/z* = 523.2 (M^+, 10 %), 440.2 ([M^+–$(CH_2)_4$NMe]$^+$, 100 %), 411.1 ([M^+–$(CH_2)_4$NMe–Et]$^+$, 100 %); Analysis. Found: C, 73.26; H, 7.08; N, 13.41; $C_{32}H_{37}N_5O_2$ requires: C, 73.39; H, 7.12; N, 13.37 %; IR (nujol, KBr): ν 3187 (N-H), 1618 (C=N), 1498 cm^{-1} (C=C).

H_2L^{NMes}: Diamine **1c** (3.34 g, 8.234 mmol), dialdehyde **2a** (2.13 g, 8.234 mmol), $BF_3{\cdot}OEt$ (1 mL), yield 77% (3.98 g, 6.331 mmol). ^{1}H NMR (599.81 MHz, $CDCl_3$): δ 8.84 (s, 2H, NH), 8.12 (s, 2H, imine), 7.03–6.98 (m, 2H, Ar-H), 6.93–6.90 (m, 4H, 2 × Ar-H), 6.80 (s, 2H, Mes-H), 6.75 (d, *J* = 8.1 Hz, 2H, Ar-H), 6.61 (d, *J* = 3.6 Hz, 2H, pyrrole), 6.29 (d, *J* = 3.6 Hz, 2H, pyrrole), 3.84 (t, *J* = 5.4 Hz, 4H, O-CH_2), 3.52 (t, *J* = 5.4 Hz, 4H, N-CH_2), 2.22 (s, 3H, *p*-Mes-CH_3), 2.20 (s, 6H, 2 × *o*-Mes-CH_3), 2.06 (q, *J* = 7.4 Hz, 4H, Et-CH_2), 0.82 (t, *J* = 7.3 Hz, 6H, Et-CH_3); ^{13}C{^{1}H} NMR (150.82 MHz, $CDCl_3$): δ 153.81 (s, CH, imine), 153.63 (s, quaternary), 145.81 (s, quaternary), 145.20 (s, quaternary), 144.12 (s, quaternary), 140.29 (s, quaternary), 137.07 (s, quaternary), 133.41 (s, quaternary), 132.13 (s, CH, Mes-H), 128.19 (s, CH, Ar-H), 124.37 (s, CH, Ar-H), 123.51 (s, CH, Ar-H), 119.13 (s, CH, pyrrole-H), 117.43 (s, CH, Ar-H), 111.92 (s, CH, pyrrole-H), 72.09 (s, CH_2, NCH_2), 56.29 (s, CH_2, OCH_2), 46.70 (s, quaternary), 31.68 (s, CH_2, Et-CH_2), 22.39 (s, CH_3, Mes-CH_3), 21.59 (s, CH_3, Mes-CH_3), 10.93 (s, CH_3, Et-CH_3); MS(EI): *m/z* = 627.3 (M^+, 8%), 408.3 ([M^+–$C_{13}H_{19}NO_2$-2(CH_3)]$^+$, 100%); Analysis. Found: 76.57; H, 7.16 N; 11.17 %; $C_{40}H_{45}N_5O_2$ requires: C, 76.52; H, 7.22; N,

11.16 %; IR (KBr, nujol): ν 3437 (N-H), 1624 (C=N), 1499 cm^{-1} (C=C).

H_2Lf^P: Diamine **1a** (1.05 g, 2.79 mmol), dialdehyde **2b** (0.982 g, 2.79 mmol), $BF_3{\cdot}OEt_2$ (0.73 mL, 5.86 mmol), yield 65% (1.26 g, 1.82 mmol). ^1H NMR (399.90 MHz, $CDCl_3$): δ 9.52 (br, s, 2H, NH), 8.17 (s, 2H, imine), 7.81 (d, *J* = 7.2 Hz, 2H, Ar-H), 7.75 (d, *J* = 7.5 Hz, 2H, Ar-H), 7.45 (td, *J* = 7.5, 1.1 Hz, 2H, Ar-H), 7.38 (td, *J* = 7.5, 1.2 Hz, 2H, Ar-H), 7.15–7.08 (m, 2H, Ar-H), 7.01–6.93 (m, 4H, 2 × Ar-H), 6.89 (dd, *J* = 8.9, 0.9 Hz, 2H, Ar-H), 6.57 (d, *J* = 3.7 Hz, 2H, pyrrole), 6.08 (d, *J* = 3.7 Hz, 2H, pyrrole), 4.18–4.14 (m, 4H, CH_2), 3.92–3.87 (m, 4H, CH_2), 3.80–3.76 (m, 4H, CH_2), 3.64–3.59 (m, 4H, CH_2); $^{13}C\{^1H\}$ NMR (125.76 MHz, $CDCl_3$): δ 151.89 (s, quaternary), 150.19 (s, CH, imine), 147.99 (s, quaternary), 141.67 (s, quaternary), 140.04 (s, quaternary), 138.83 (s, quaternary), 131.56 (s, quaternary), 128.66 (s, CH, Ar-H), 128.28 (s, CH, Ar-H), 126.13 (s, CH, Ar-H), 125.86 (s, CH, Ar-H), 121.65 (s, CH, Ar-H), 120.74 (s, CH, Ar-H), 119.97 (s, CH, Ar-H), 117.18 (s, CH, Ar-H), 112.77 (s, CH, pyrrole), 110.26 (s, CH, pyrrole), 71.65 (s, CH_2, OCH_2), 70.84 (s, CH_2, OCH_2), 69.72 (s, CH_2, OCH_2), 69.21 (s, CH_2, OCH_2), 58.59 (s, quaternary); MS(EI): 692.2 (M^+, 100%), 545.3 ($[M^+$–fluorenyl$]^+$, 30 %); Analysis. Found: C, 74.42; H, 5.96; N, 7.94; $C_{43}H_{40}N_4O_5$ requires: C, 74.55; H, 5.82; N, 8.09 %; IR (nujol, KBr): ν 3211 (N-H), 1620 (C=N), 1492 cm^{-1}(C=C).

H_2Lf^{NMe}: Diamine **1b** (1.04 g, 3.44 mmol), dialdehyde **2b** (1.213 g, 3.44 mmol), $BF_3{\cdot}OEt_2$ (0.91 mL, 7.22 mmol), yield 70 % (1.49 g, 2.41 mmol). ^1H NMR (500.12 MHz,$CDCl_3$): δ 9.50 (br, s, 2H, NH), 8.16 (s, 2H, imine), 7.93 (d, *J* = 7.3 Hz, 2H, Ar-H), 7.81 (d, *J* = 7.3 Hz, 2H, Ar-H), 7.44 (td, *J* = 7.4, 1.1 Hz, 2H, Ar-H), 7.38 (td, *J* = 7.4, 1.3 Hz, 2H, Ar-H), 7.34 (td, *J* = 7.6, 1.8 Hz, 2H, Ar-H), 7.01 (m, 4H, Ar-H), 6.51 (d, *J* = 3.8 Hz, 2H, pyrrole CH), 5.83 (d, 3.8 Hz, 2H, pyrrole CH), 4.22 (m, 4H, CH_2), 3.08 (m, 4H, CH_2), 2.64 (s, 3H, N-CH_3); $^{13}C\{^1H\}$ NMR (125.76 MHz, $CDCl_3$): δ 151.10 (s, CH, imine), 150.99 (s, quaternary), 147.42 (s, quaternary), 146.44 (s, quaternary), 142.40 (s, quaternary), 139.80 (s, quaternary), 132.01 (s, quaternary), 128.38 (s, CH, Ar-H), 127.96 (s, CH, Ar-H), 125.90 (s, CH, Ar-H), 125.38 (s, CH, Ar-H), 121.75 (s, CH, Ar-H), 120.91 (s, CH, Ar-H), 120.60 (s, CH, Ar-H), 116.70 (s, CH, Ar-H), 113.57 (s, CH, pyrrole), 109.66 (s, CH, pyrrole), 68.42(s, CH_2, O/N-CH_2), 66.99 (s, CH_2, O/N-CH_2), 55.91 (s, quaternary), 43.21 (s, CH_3, NCH_3); MS(EI): 617.2 (M^+, 20 %), 534.2 ($[M^+$–$(C_4H_8NMe)]^+$, 100 %); Analysis. Found: C, 77.64; H, 5.59; N, 11.28; $C_{40}H_{35}N_5O_2$ requires: C, 77.77; H, 5.71; N, 11.34 %; IR (nujol, KBr): ν 3197 (N-H), 1621 (C=N), 1502 cm^{-1} (C=C).

Crystallographic issues: Protons of the water could not be located in the difference Fourier map and thus are not present in the structure, but are accounted for in the chemical formula, mass etc.

Potassium and magnesium complexes

$K_2(L^P)$: A mixture of H_2L^P (0.15g, 0.25 mmol) and excess KH (26 mg, 0.66 mol) was treated with THF (5 mL). Gas evolved immediately, and the mixture stirred for 3 h at room temperature giving a red solution from which $K_2(L^P)$ as an orange solid (0.16 g, 0.24 mmol, 95 %) precipitated on addition of hexane (10 mL).

Crystals suitable for X-ray crystallography of $K_2(L^P)$ were grown by hexane diffusion in to a THF solution. ^{1}H NMR (399.90 MHz, C_6D_6/H_8-THF): δ 8.35 (s, 2H, imine), 7.39 (d, *J* = 7.4 Hz, 2H, Ar-H), 7.17–7.01 (m, 6H, Ar-H), 6.83 (d, *J* = 3.1 Hz, 2H, pyrrole), 6.39 (d, *J* = 3.1 Hz, 2H, pyrrole), 4.31 (s, 4H, OCH_2), 2.52 (q, *J* = 7.2 Hz, 4H, Et-CH_2), 1.06 (t, *J* = 7.3 Hz, 6H, Et-CH_3) [NB Other OCH_2 resonances masked by suppressed THF]; $^{13}C\{^1H\}$ NMR (100.55 MHz, C_6D_6/H_8-THF): δ 161.67 (s, quaternary), 152.92 (s, quaternary), 152.06 (s, CH, imine), 145.21 (s, quaternary), 138.98 (s, quaternary), 122.34 (s, CH, Ar-H), 121.77 (s, CH, Ar-H), 120.30 (s, CH, Ar-H), 116.94 (s, CH, Ar-H), 113.01 (s, CH, pyrrole), 108.19 (s, CH, pyrrole), 72.05 (s, CH_2, OCH_2), 66.53 (s, CH_2, OCH_2), 65.83 (s, CH_2, OCH_2), 65.75 (s, CH_2, OCH_2), 48.40 (s, quaternary), 29.05 (s, CH_2, Et-CH_2), 9.14 (s, CH_3, Et-CH_3); MS(EI): *m/z* = 674.3 (M^+, 75 %), 646.1 ($[M^+–Et]^+$, 100 %, 607.2 ($[M^+–K–Et]^+$, 78 %); Analysis. Found:. C, 62.18; H, 5.87; N, 8.18; $C_{35}H_{40}K_2N_4O_5$ requires: C, 62.29; H, 5.97; N, 8.30 %; IR (nujol, KBr): ν 1557 (C=N), 1502 cm^{-1} (C=C).

$K_2(L^{NMe})$: H_2L^{NMe} (0.21g, 0.40 mmol), KH (48 mg, 1.2 mmol), Yield 96 % orange solid (0.23 g, 0.38 mmol). ^{1}H NMR (399.90 MHz, C_6D_6/H_8-THF): δ 8.31 (s, 2H, imine), 7.29–7.23 (m, 2H, Ar-H), 7.20–7.04 (m, 6H, Ar-H), 6.81 (d, *J* = 3.0 Hz, 2H, pyrrole), 6.40 (d, *J* = 3.1 Hz, 2H, pyrrole), 4.35–4.27 (m, 4H, O/N-CH_2), 3.03 (s, 4H, O/N-CH_2), 2.59 (s, 3H, N-CH_3), 1.10 (t, *J* = 7.3 Hz, 3H, Et-CH_3) [Et-CH_2 resonance masked by suppressed THF]; $^{13}C\{^1H\}$ NMR (100.55 MHz, C_6D_6/H_8-THF): δ 159.68 (s, quaternary), 154.71 (s, quaternary), 152.35 (s, CH, imine), 146.33 (s, quaternary), 138.30 (s, quaternary), 122.34 (s, CH, Ar-H), 121.98 (s, CH, Ar-H), 119.21 (s, CH, Ar-H), 118.55 (s, CH, Ar-H), 113.76 (s, CH, pyrrole), 108.23 (s, CH, pyrrole), 65.82 (s, CH_2, O/N-CH_2), 56.95 (s, CH_2, O/N-CH_2), 47.69 (s, quaternary), 45.05 (s, CH_3, NCH_3), 30.98 (s, CH_2, Et-CH_2), 9.65 (s, CH_3, Et-CH_3); MS(EI): *m/z* = 599.3 ($M^{+\cdot}$, 4%), 570 ($[M^+–Et]^+$, 50 %), 561.2 ($[M^+–K]^+$, 15 %), 532.3 ($[M^+–K–Et]^+$, 100%); Analysis. Found: C, 63.97; H, 6.01; N, 11.59; $C_{32}H_{35}K_2N_5O_2$ requires: C, 64.07; H, 5.88; N, 11.68 %; IR (nujol, KBr): ν 1565 (C=N), 1499 cm^{-1} (C=C).

$K_2(Lf^P)$: H_2Lf^P (50 mg, 0.072 mmol), KH (9 mg, 0.22 mmol), yield 94 % red powder (52 mg, 0.068 mmol). ^{1}H NMR (399.90 MHz, C_6D_6/H_8-THF): δ 8.42 (s, 2H, imine), 8.31 (d, *J* = 7.1 Hz, 2H, Ar-H), 8.00 (d, *J* = 7.1 Hz, 2H, Ar-H), 7.57–7.47 (m, 6H, Ar-H), 7.45 (d, *J* = 7.2 Hz, 2H, Ar-H), 7.28 (d, *J* = 3.5 Hz, 2H, Ar-H), 7.23–7.18 (m, 2H, Ar-H), 6.75 (d, *J* = 3.1 Hz, 2H, pyrrole), 6.03 (d, *J* = 3.0 Hz, 2H, pyrrole) [OCH_2 not seen due to THF suppression]; $^{13}C\{^1H\}$ NMR (125.76 MHz, C_6D_6/H_8-THF): δ 154.28 (s, quaternary), 152.90 (s, quaternary), 152.47 (s, CH, imine), 145.10 (s, quaternary), 141.00 (s, quaternary), 139.70 (s, quaternary), 128.19 (s, CH, Ar-H), 126.27 (s, CH, Ar-H), 125.91 (s, CH, Ar-H), 122.42 (s, CH, Ar-H), 122.22 (s, CH, Ar-H), 119.67 (s, CH, Ar-H), 119.19 (s, CH, Ar-H), 117.14 (s, CH, Ar-H), 113.30 (s, CH, pyrrole), 108.83 (s, CH, pyrrole), 69.96 (s, CH_2, OCH_2), 66.82 (s, CH_2, OCH_2), 65.83 (s, CH_2, OCH_2), 65.41 (s, CH_2, OCH_2); MS(EI): *m/z* = 768.1 ($M^{+\cdot}$, 55 %), 730.2 ($[M^+-K]^+$, 100%); IR (nujol, KBr): ν 1563 (C=N), 1499 cm^{-1} (C=C).

$K_2(Lf^{NMe})$: H_2Lf^{NMe} (52 mg, 0.084 mmol), KH (10 mg, 0.25 mmol), yield 89 % red powder (52 mg, 0.075 mmol). ^{1}H NMR (399.90 MHz, C_6D_6/H_8-THF): δ 8.01 (s, 2H, imine), 7.71 (d, *J* = 7.4 Hz, 2H, Ar-H), 7.64 (d, *J* = 7.4 Hz, 2H, Ar-H), 7.15 (t, *J* = 7.3 Hz, 2H, Ar-H), 7.07 (t, *J* = 7.3 Hz, 2H, Ar-H), 6.99–6.93 (m, 2H, Ar-

H), 6.87–6.82 (m, 2H, Ar-H), 6.82–6.74 (m, 4H, Ar-H), 6.31 (d, J = 3.1 Hz, 2H, pyrrole), 5.45 (d, J = 3.1 Hz, 2H, pyrrole), 4.03–3.96 (m, 4H, CH_2), 2.75–2.67 (m, 4H, CH_2) [NCH_3 not seen due to THF suppression]; $^{13}C\{^1H\}$ NMR (125.76 MHz, C_6D_6/H_8-THF): δ 155.20 (s, quaternary), 154.75 (s, CH, imine), 154.21 (s, quaternary), 151.91 (s, quaternary), 145.83 (s, quaternary), 140.62 (s, quaternary), 138.73 (s, quaternary), 127.07 (s, CH, Ar-H), 125.96 (s, CH, Ar-H), 125.70 (s, CH, Ar-H), 122.31 (s, CH, Ar-H), 121.67 (s, CH, Ar-H), 119.01 (s, CH, Ar-H), 118.97 (s, CH, Ar-H), 118.30 (s, CH, pyrrole), 113.52 (s, CH, Ar-H), 108.40 (s, CH, pyrrole), 66.84 (s, CH_2, O/N-CH_2), 64.35 (s, quaternary), 56.46 (s, CH_2, O/N-CH_2), 44.79 (s, CH_3, NCH_3); MS(EI): *m/z* = 693.1 ($M^{+\cdot}$, 10 %), 655.2 ($[M^+–K]^+$, 100%); Analysis. Found: C, 69.23; H, 4.68; N, 9.97; $C_{40}H_{33}K_2N_5O_2$ requires: C, 69.23; H, 4.79; N, 10.09 %; IR (nujol, KBr): ν 1565 (C=N), 1510 cm^{-1} (C=C)

Mg(L^P): A 1.0 M solution of Mg^nBu_2 in heptane (1 mL, 1.0 mmol) was added dropwise to a stirring solution of H_2L^P (0.600 g, 1.0 mmol) in THF (10 mL) at -80 °C. The solution was allowed to warm to room temperature and stirred for 3 h during which a colour changed from yellow/orange to a dichroic bright yellow solution was observed, after which the solvent volume was reduced under vacuum and Mg(L^P) precipitated with hexane (5 mL) giving Mg(L^P) as a yellow solid (0.590 g, 0.95 mmol, 95 %). ^1H NMR (500.12 MHz, C_6D_6): δ 8.23 (s, 2H, imine), 7.16–7.15 (m, 2H, pyrrole), 6.92–6.83 (m, 6H, 3 × Ar-H), 6.65 (d, J = 3.5 Hz, 2H, pyrrole), 6.63–6.60 (m, 2H, Ar-H), 3.78–3.71 (m, 2H, OCH_2), 3.71–3.64 (m, 2H, OCH_2), 3.44 (d, J = 12.3 Hz, 2H, OCH_2), 3.37–3.29 (m, 4H, 2 × O-CH_2), 3.21–3.13 (m, 2H, O-CH_2), 3.07 (dd, J = 11.1, 1.7 Hz, 2H, OCH_2), 2.94–2.85 (m, 2H, OCH_2), 2.38 (q, J = 7.3 Hz, 2H, Et-CH_2), 2.12 (q, J = 7.3 Hz, 2H, Et-CH_2), 1.16 (t, J = 7.2 Hz, 3H, Et-CH_3), 0.89 (t, J = 7.4 Hz, 3H, Et-CH_3); $^{13}C\{^1H\}$ NMR (125.76 MHz, C_6D_6): δ 156.98 (s, quaternary), 156.58 (s, CH, imine), 151.62 (s, quaternary), 143.54 (s, quaternary), 136.48 (s, quaternary), 123.59 (s, CH, Ar-H), 122.92 (s, CH, Ar-H), 122.43 (s, CH, Ar-H), 120.03 (s, CH, pyrrole), 116.75 (s, CH, Ar-H), 111.67 (s, CH, pyrrole), 71.04 (s, CH_2, OCH_2), 70.72 (s, CH_2, OCH_2), 70.63 (s, CH_2, OCH_2), 70.24 (s, CH_2, OCH_2), 48.55 (s, quaternary), 41.47 (s, CH_2, Et-CH_2), 34.33 (s, CH_2, Et-CH_2), 11.48 (s, CH_3, Et-CH_3), 10.52 (s, CH_3, Et-CH_3). MS(EI): *m/z* = 621.2 (M^+, 8%), 592.1 ($[M^+–Et]^+$, 100 %); Analysis. Found: C, 67.64; H, 6.37; N, 8.93; $C_{35}H_{40}N_4O_5Mg$ requires: C, 67.69; H, 6.49; N, 9.02 %; IR (nujol, KBr): ν 1564 (C=N), 1506 cm^{-1} (C=C).

Mg(L^{NMe}): Mg^nBu_2 in heptane (1.0 M, 1.2 mL, 1.2 mmol), H_2L^{NMe} (0.628 g, 1.2 mmol), yield 93 % yellow solid (0.609 g, 0.112 mmol). ^1H NMR (500.12 MHz, C_6D_6): δ 8.20 (s, 2H, imine), 7.13 (d, J = 3.5 Hz, 2H, pyrrole), 6.90–6.83 (m, 4H, 2 × Ar-H), 6.67 (d, J = 4.5 Hz, 2H, Ar-H), 6.60 (d, J = 3.5 Hz, 2H, pyrrole), 6.52 (d, J = 8.1 Hz, 2H, Ar-H), 3.61–3.53 (m, 2H, O/N-CH_2), 3.03 (s, 2H, O/N-CH_2), 2.46–2.38 (m, 2H, O/N-CH_2), 2.31–2.21 (m, 4H, 2 × Et-CH_2), 2.06 (s, 3H, N-CH_3), 2.09–2.00 (m, 2H, O/N-CH_2), 0.97–0.89 (m, 3H, Et-CH_3), 0.89–0.80 (m, 3H, Et-CH_3); $^{13}C\{^1H\}$ NMR (125.76 MHz, C_6D_6): δ 158.57 (s, CH, imine), 157.27 (s, quaternary), 152.38 (s, quaternary), 142.13 (s, quaternary), 134.95 (s, quaternary), 123.55 (s, CH, Ar), 122.36 (s, CH, Ar), 120.97 (s, CH, Ar), 120.33 (s, CH, pyrrole), 114.58 (s, Ar-H), 110.96 (s, CH, pyrrole), 57.47 (s, quaternary), 55.48 (s, CH_2, O/N-CH_2), 48.83 (s, CH_2, O/N-CH_2), 45.60 (s, CH_3, N-CH_3), 38.67 (s, CH_2, Et-

CH_2), 38.03 (s, CH_2, Et-CH_2), 10.48 (s, CH_3, Et-CH_3), 10.19 (s, CH_3, Et-CH_3); MS(EI): 584.3 ($[M^+ + K]^+$, 10 %), 551.2 ($[M^+ + Li]^+$, 50 %), 503 ($[M^+ – Et – Me]^+$, 100 %); Analysis. Found: C, 70.31; H, 6.53; N, 12.87; $C_{32}H_{35}MgN_5O_2$ requires: C, 70.40; H, 6.46; N, 12.83 %; IR (nujol, KBr): ν 1569 (C=N), 1490 cm^{-1} (C=C).

Mg(Lf^P): $Mg(^nBu)_2$ in heptane (0.5 M, 0.48 mL, 0.244 mmol), H_2Lf^P (0.169 g, 0.244 mmol), yield 95 % yellow solid (0.166 g, 0.232 mmol). ^1H NMR (500.12 MHz, C_6D_6): δ 8.23 (d, *J* = 8.1 Hz, 1H, Ar^F-H), 8.21 (s, 2H, imine), 7.80 (d, *J* = 6.9 Hz, 1H, Ar^F-H), 7.67 (d, *J* = 7.5 Hz, 1H, Ar^F-H), 7.58 (d, *J* = 6.8 Hz, 1H, Ar^F-H), 7.46 (d, *J* = 7.5 Hz, 1H, Ar^F-H), 7.41–7.33 (m, 2H, Ar^F-H), 7.12 (t, *J* = 7.1 Hz, 1H, Ar^F-H), 7.01–6.98 (m, 2H, Ar-H), 6.97–6.93 (m, 4H, Ar-H), 6.81 (d, *J* = 3.5 Hz, 2H, pyrrole), 6.70–6.67 (m, 2H, Ar-H), 5.97 (d, *J* = 3.4 Hz, 2H, pyrrole), 3.44–3.14 (m, 14H, OCH_2), 2.77 (t, *J* = 9.7 Hz, 2H, OCH_2); $^{13}C\{^1H\}$ NMR (125.76 MHz, C_6D_6): δ 156.58 (s, CH, imine), 155.20 (s, quaternary), 153.65 (s, quaternary), 152.61 (s, quaternary), 151.52 (s, quaternary), 143.36 (s, quaternary), 142.34 (s, quaternary), 138.67 (s, quaternary), 136.84 (s, quaternary), 127.27 (s, CH, Ar-H), 127.24 (s, CH, Ar-H), 126.95 (s, CH, Ar-H), 126.53 (s, CH, Ar-H), 126.00 (s, CH, Ar-H), 124.59 (s, CH, Ar-H), 123.53 (s, CH, Ar-H), 122.55 (s, CH, Ar-H), 122.30 (s, CH, Ar-H), 120.06 (s, CH, Ar-H), 119.96 (s, CH, Ar-H), 119.75 (s, CH, pyrrole), 116.63 (s, CH, Ar-H), 111.51 (s, CH, pyrrole), 71.15 (s, CH_2, OCH_2), 70.34 (s, CH_2, OCH_2), 70.26 (s, CH_2, OCH_2), 69.94 (s, CH_2, OCH_2), 59.66 (s, quaternary); MS(EI): *m/z* = 714.2 ($M^{+\cdot}$, 100 %); IR (nujol, KBr): ν 1567 (C=N), 1482 cm^{-1} (C=C).

Mg(Lf^{NMe}): $Mg(^nBu)_2$ in heptane (0.5 M, 0.67 mL, 0.336 mmol), H_2Lf^{NMe} (0.207 g, 0.336 mmol), yield 93 % yellow solid (0.200 g, 0.312 mmol). ^1H NMR (500.12 MHz, C_6D_6): δ 8.22 (s, 2H, imine), 7.70 (br, s, 2H, Ar-H), 7.47 (d, *J* = 7.4 Hz, 2H, Ar-H), 7.32–6.99 (m, 8H, Ar-H), 6.90–6.84 (m, 2H, Ar-H), 6.79 (d, *J* = 3.5 Hz, 2H, pyrrole), 6.69–6.65 (m, 4H, Ar-H), 6.47 (d, *J* = 8.1 Hz, 2H, Ar-H), 5.97 (d, *J* = 3.5 Hz, 2H, pyrrole), 3.56 (br, s, 2H, CH_2), 3.14 (br, s, 2H, CH_2), 2.45 (br, s, *J* = 21.3 Hz, 2H, CH_2), 2.13 (br, s, 2H, CH_2), 1.94 (s, 3H, N-CH_3); $^{13}C\{^1H\}$ NMR (125.76 MHz, C_6D_6): δ 159.57 (s, CH, imine), 153.82 (s, quaternary), 151.94 (s, quaternary), 141.55 (s, quaternary), 136.12 (s, quaternary), 128.19 (s, quaternary), 127.98 (s, quaternary), 127.79 (s, quaternary), 127.60 (s, quaternary), 126.86 (s, CH, Ar-H),126.82 (s, CH, Ar-H), 126.78 (s, CH, Ar-H), 126.60 (s, CH, Ar-H), 126.41 (s, CH, Ar-H), 124.69 (s, CH, Ar-H), 123.91 (s, CH, Ar-H), 122.69 (s, CH, Ar-H), 120.71 (s, CH, Ar-H), 120.11 (s, CH, Ar-H), 119.91 (s, CH, Ar-H), 119.76 (s, CH, pyrrole), 113.77 (s, CH, Ar-H), 112.19 (s, CH, pyrrole), 67.44 (s, CH_2, OCH_2), 59.34 (s, quaternary), 54.79 (s, CH_2, NCH_2), 45.00 (s, CH_3, NCH_3); MS(EI): *m/z* = 639.1 (M^+, 15 %), 626.2 ($[M^+ – Me]^+$, 100 %). IR (nujol, KBr): ν 1557 (C=N), 1496 cm^{-1} (C=C).

Palladium complexes

Pd(L^P): A mixture of H_2L^P (0.100 g, 0.167 mmol) and $Pd(OAc)_2$ (37.5 mg, 0.167 mmol) in toluene (*ca*. 10 mL) was stirred for 30 min. The resulting red/brown mixture was treated with NEt_3 (56 µl). The reaction was stirred overnight, filtered and solvents removed under vacuum. The product was extracted into hexane (3 × 10

mL) to give pure Pd(L^P) as a yellow solid (79 mg, 0.112 mmol, 67 %). ^{1}H NMR (391.79 MHz, $CDCl_3$): δ 7.55 (s, 2H, imine), 6.83 (d, 2H, *J* = 4.0 Hz, pyrrole), 6.78 (m, 2H, Ar-H), 6.71 (m, 2H, Ar-H), 6.38 (m, 2H, Ar-H), 6.34 (m, 2H, Ar-H), 6.11 (d, 2H, *J* = 4.0 Hz, pyrrole), 4.05 (m, 2H, OCH_2), 3.83–3.32 (m, 14H, OCH_2), 2.05 (q, 2H, *J* = 7.2 Hz, Et-CH_2), 2.01 (q, 2H, *J* = 7.3 Hz, Et-CH_2), 0.45 (t, 3H, *J* = 7.1 Hz, Et-CH_3), 0.42 (t, 3H, *J* = 7.3 Hz, Et-CH_3); $^{13}C\{^1H\}$ NMR (98.51 MHz, $CDCl_3$): δ 160.0 (s, CH, imine), 151.2 (s, quaternary), 148.5 (s, quaternary), 138.0 (s, quaternary), 136.7 (s, quaternary), 125.9 (s, CH, Ar-H), 124.3 (s, CH, Ar-H), 120.4 (s, CH, Ar-H), 118.7 (s, CH, Ar-H), 111.1 (s, CH, pyrrole), 107.3 (s, CH, pyrrole), 71.0 (s, CH_2, OCH_2), 70.5 (s, CH_2, OCH_2), 69.6 (s, CH_2, OCH_2), 68.2 (s, CH_2, OCH_2), 53.8 (s, quaternary), 38.3 (s, CH_2, Et-CH_2), 37.6 (s, CH_2, Et-CH_2), 9.9 (s, CH_3, Et-CH_3); MS(EI): *m/z* = 702.1 (M^+, 4 %), 673.0 ($[M^+–Et]^+$, 100 %); Analysis. Found: C, 59.94; H, 5.69; N, 8.00; $C_{35}H_{40}N_4O_5Pd$ requires: C, 59.79; H, 5.73; N, 7.97 %; IR (nujol, KBr): ν 1557 (C=N), 1496 cm^{-1} (C=C).

Pd(L^{NMe}): H_2L^{NMe} (0.500 g, 0.954 mmol), $Pd(OAc)_2$ (0.214 g, 0.954 mmol), toluene (*ca*. 30 mL), NEt_3 (0.30 mL), yield 73 % yellow solid (0.44 g, 0.70 mmol). Crystals suitable for X-ray crystallography were grown from a saturated hexane solution. ^{1}H NMR (391.79 MHz, $CDCl_3$): δ 7.54 (s, 2H, imine), 6.92 (d, 2H, *J* = 3.9 Hz, pyrrole), 6.87 (m, 2H, Ar-H), 6.75 (d, *J* = 7.7 Hz, Ar-H), 6.47 (m, 4H, Ar-H), 6.20 (d, *J* = 3.6 Hz, pyrrole), 4.06 (m, 2H, O/N-CH_2), 3.60 (m, 2H, O/N-CH_2), 3.02 (m, 2H, O/N-CH_2), 2.85 (m, 2H, O/N-CH_2), 2.43 (s, 3H, N-CH_3), 2.16 (q, 2H, *J* = 7.4 Hz, Et-CH_2), 2.07 (q, 2H, *J* = 7.2 Hz, Et-CH_2), 0.56 (t, 3H, *J* = 7.1 Hz, Et-CH_2), 0.53 (t, 3H, *J* = 7.5 Hz, Et-CH_2); $^{13}C\{^1H\}$ NMR (98.51 MHz): δ 160.0 (s, CH, imine), 151.2 (s, quaternary), 148.6 (s, quaternary), 138.8 (s, quaternary), 136.5 (s, quaternary), 125.9 (s, CH, Ar-H), 124.1 (s, CH, Ar-H), 120.5 (s, CH, Ar-H), 118.7 (s, CH, Ar-H), 112.7 (s, CH, pyrrole), 107.4 (s, CH, pyrrole), 68.0 (s, CH_2, O/N-CH_2), 55.2 (s, CH_2, O/N-CH_2), 53.7 (s, quaternary), 46.5 (s, CH_2, Et-CH_2), 38.7 (s, CH_3, N-CH_3), 37.0 (s, CH_2, Et-CH_2), 10.0 (s, CH_3, Et-CH_3), 9.7 (s, CH_3, Et-CH_3); MS(EI): *m/z* = 627.1 (M^+, 9 %), 598.0 ($[M^+–Et]^+$, 100 %). Analysis. Found: C, 61.20; H, 5.66; N, 11.07. $C_{32}H_{35}N_5O_2Pd$ requires: C, 61.19; H, 5.62; N, 11.15 %; IR (nujol, KBr): ν 1562 (C=N), 1496 cm^{-1} (C=C).

Pd(L^{NMes}): H_2L^{NMes} (0.20 g, 3.20 mmol), $Pd(OAc)_2$ (0.072 g, 3.20 mmol),toluene (20 mL), NEt_3 (0.032 g, 0.023 mL), yield yellow solid 68 % (0.15 g, 0.22 mol). ^{1}H NMR (500.12 MHz, $CDCl_3$): δ 7.54 (s, 2H, imine), 6.96 (d, *J* = 3.9 Hz, 2H, pyrrole), 6.93–6.89 (m, 2H, Ar-H), 6.84 (s, 1H, Mes-H), 6.79 (dd, *J* = 7.7 Hz, 2H, Ar-H), 6.78 (s, 1H, Mes-H), 6.51–6.45 (m, 4H, 2 × Ar-H), 6.21 (d, *J* = 3.9 Hz, 2H, pyrrole), 4.09–4.02 (m, 2H, N/OCH_2), 3.77–3.69 (m, 4H, N/OCH_2), 3.22–3.14 (m, 2H, N/OCH_2), 2.23 (s, 3H, Mes-CH_3), 2.20 (s, 3H, Mes-CH_3), 2.17 (q, *J* = 7.1 Hz, 2H, Et-CH_3), 2.10 (s, 3H, Mes-CH_3), 2.07 (q, *J* = 7.1 Hz, 2H, Et-CH_2), 0.58 (t, *J* = 7.2 Hz, 3H, Et-CH_3), 0.51 (t, *J* = 7.2 Hz, 3H, Et-CH_3); $^{13}C\{^1H\}$ NMR (125.76 MHz, $CDCl_3$): δ 159.90 (s, CH, imine), 151.27 (s, quaternary), 148.53 (s, quaternary), 147.61 (s, quaternary), 138.31 (s, quaternary), 136.95 (s, quaternary), 136.35 (s, quaternary), 136.34 (s, quaternary), 134.83 (s, quaternary), 130.29 (s, CH, Ar-H), 128.76 (s, CH, Ar-H), 125.87 (s, CH, Ar-H), 123.88 (s, CH, Ar-H), 120.21 (s, CH, Ar-H), 118.65 (s, CH, Ar-H), 111.97 (s, CH, Ar-H), 107.24 (s, CH, Ar-H), 69.94 (s, CH_2, O/N-CH_2), 53.76 (s, quaternary),

53.51 (s, CH_2, O/N-CH_2), 38.90 (s, CH_2, Et-CH_2), 36.74 (s, CH_2, Et-CH_2), 20.71 (s, CH_3, Ar-CH_3), 19.14 (s, CH_3, Ar-CH_3), 18.80 (s, CH_3, Ar-CH_3), 9.93 (s, CH_3, Et-CH_3), 9.46 (s, CH_3, Et-CH_3); MS(EI): *m/z* = 731.2 (M^+, 3%), 702.1 ($[M^+–2(CH_3)]^+$, 100%); Analysis. Found: 65.54; H, 5.97; N, 9.50; $C_{40}H_{43}N_5O_2Pd$ requires: C, 65.61; H, 5.92; N, 9.56 %; IR (KBr, nujol): ν 1560 (C=N), 1497 cm^{-1} (C=C).

Pd(Lf^P): H_2L^{FP} (0.200 g, 0.289 mmol), $Pd(OAc)_2$ (65 mg, 0.289 mmol),CH_2Cl_2 (10 mL), NEt_3 (0.09 mL, 0.61 mmol), yield 35 % yellow solid (81 mg, 0.101 mmol) ^1H NMR (399.90 MHz, $CDCl_3$): δ 7.78 (dd, *J* = 7.8, 1.7 Hz, 2H, Ar-H), 7.63 (s, 2H, imine), 7.42–7.33 (m, 2H, Ar-H), 7.31 (d, *J* = 7.4 Hz, 2H, Ar-H), 7.16 (dt, *J* = 7.8, 1.7 Hz, 2H, Ar-H), 6.89 (dt, *J* = 7.8, 1.6 Hz, 2H, Ar-H), 6.82 (dd, *J* = 7.7, 1.6 Hz, 2H, Ar-H), 6.63 (d, *J* = 3.9 Hz, 2H, pyrrole), 6.52–6.44 (m, 4H, Ar-H), 5.43 (d, *J* = 3.9 Hz, 2H, pyrrole), 4.24–4.14 (m, 2H, CH_2), 3.96–3.87 (m, 4H, CH_2), 3.77–3.67 (m, 6H CH_2), 3.64–3.58 (m, 2H CH_2), 3.54–3.47 (m, 2H CH_2); $^{13}C\{^1H\}$ NMR (125.76 MHz, $CDCl_3$): δ 160.63 (s, CH, imine), 151.34 (s, quaternary), 150.55 (s, quaternary), 149.83 (s, quaternary), 145.92 (s, quaternary), 140.93 (s, quaternary), 140.37 (s, quaternary), 137.78 (s, quaternary), 137.73 (s, quaternary), 128.31 (s, CH, Ar-H), 128.01 (s, CH, Ar-H), 127.90 (s, CH, Ar-H), 127.55 (s, CH, Ar-H), 126.30 (s, CH, Ar-H), 125.51 (s, CH, Ar-H), 124.67 (s, CH, Ar-H), 124.16 (s, CH, Ar-H), 120.49 (s, CH, Ar-H), 120.30 (s, CH, Ar-H), 120.13 (s, CH, Ar-H), 118.51 (s, CH, Ar-H), 111.39 (s, CH, pyrrole), 108.59 (s, CH, pyrrole), 71.29 (s, CH_2, OCH_2), 70.59 (s, CH_2, OCH_2), 69.68 (s, CH_2, OCH_2), 68.23 (s, CH_2, OCH_2), 61.56 (s, quaternary); MS(EI): *m/z* = 796.2 (M^+, 100%); Analysis. Found:. C, 64.73; H, 6.37; N, 6.94; $C_{43}H_{38}N_4O_5Pd$ requires: C, 64.78; H, 4.80; N, 7.03 %; IR (nujol, KBr): ν 1552 (C=N), 1496 cm^{-1} (C=C).

Pd(Lf^{NMe}): H_2L^{FNMe} (0.213 g, 0.345 mmol), $Pd(OAc)_2$ (81 mg, 0.345 mmol), CH_2Cl_2 (10 mL), NEt_3 (1.1 mL, 0.796 mmol), yield 42 % yellow solid (0.104 g, 0.145 mmol). ^1H NMR (500.12 MHz, $CDCl_3$): δ 7.82 (t, *J* = 7.0 Hz, 2H, Ar-H), 7.57 (s, 2H, imine), 7.46–7.35 (m, 4H, Ar-H), 7.29–7.23 (m, 2H, Ar-H), 6.96 (td, *J* = 7.9, 1.6 Hz, 2H, Ar-H), 6.83 (dd, *J* = 7.9, 1.6 Hz, 2H, Ar-H), 6.68 (d, *J* = 3.9 Hz, 2H, pyrrole), 6.58–6.53 (m, 4H, Ar-H), 5.48 (d, *J* = 3.9 Hz, 2H, pyrrole), 4.28–4.22 (m, 2H, CH_2), 3.89–3.82 (m, 2H, CH_2), 3.39–3.31 (m, 2H, CH_2), 3.31–3.24 (m, 2H, CH_2), 2.66 (s, 3H, N-CH_3); $^{13}C\{^1H\}$ NMR (125.76 MHz, $CDCl_3$): δ 160.55 (s, CH, imine), 150.38 (s, quaternary), 149.93 (s, quaternary), 149.72 (s, quaternary), 146.02 (s, quaternary), 140.63 (s, quaternary), 140.41 (s, quaternary), 138.14 (s, quaternary), 137.43 (s, quaternary), 128.17 (s, CH, Ar-H), 128.09 (s, CH, Ar-H), 127.73 (s, CH, Ar-H), 127.57 (s, CH, Ar-H), 126.35 (s, CH, Ar-H), 125.15 (s, CH, Ar-H), 124.93 (s, CH, Ar-H), 123.98 (s, CH, Ar-H) , 120.78 (s, CH, Ar-H), 120.13 (s, CH, Ar-H), 120.07 (s, CH, Ar-H), 118.65 (s, CH, Ar-H), 112.35 (s, CH, pyrrole), 108.61 (s, CH, pyrrole), 65.85 (s, CH_2, O/N-CH_2), 61.44 (s, quaternary), 54.41 (s, CH_2, O/N-CH_2), 45.40 (s, CH_3, NCH_3); MS(EI): *m/z* = 721.1 (M^+, 87 %), 638.0 ($[M^+–O(CH_2)_2N(CH_3)(CH_2)_2O]^+$, 100 %); Analysis. Found: C, 66.67; H, 4.62; N, 9.71; $C_{40}H_{33}N_5O_2Pd$ requires: C, 66.53; H, 4.61; N, 9.70 %; IR (nujol, KBr): ν 1562 (C=N), 1504 cm^{-1} (C=C).

Titanium, vanadium, and chromium complexes

TiCl(L^P): A mixture of H_2L^P (0.438 g, 0.732 mmol) and excess KH (90 mg, 2.2 mmol) was treated with THF

(30 mL). Gas evolved immediately, and, once effervescence had ceased, the mixture was filtered on a stirred suspension of $TiCl_3(THF)_3$ (0.271 g, 0.732 mmol) in THF (10 mL) at -80 °C. A rapid colour change from red to dark brown was observed and the reaction was warmed to room temperature and left to stir for 2 h. The mixture was filtered through Celite, the Celite was washed with THF (3 × 5 mL) and solvents removed under vacuum giving $TiCl(L^P)$ as a brown solid (0.22 g, 0.30 mmol, 45 %). Crystals of $TiCl(L^P)$ suitable for X-ray crystallography were grown by hexane diffusion into a THF solution. MS(EI): *m/z* = 679.2 (M^+, 35 %), 631.2 ($[M^+–Cl–Me]^+$, 100 %), 616.2 ($[M^+–Et–Cl]^+$, 40 %); Analysis. Found: C, 61.70; H, 6.05; N, 8.16; $C_{35}H_{40}ClN_4O_5Ti$ requires: C, 61.82; H, 5.93; N, 8.24 %; IR (nujol, KBr): ν 1579 (C=N), 1520 cm^{-1} (C=C).

Crystallographic issues: Attempts to model the apparent disorder in THF solvent of crystallisation and the polyether backbone (around C26) were unsuccessful and led to diverging structures.

$TiCl(L^{NMe})$: H_2L^{NMe} (0.499 g, 0.952 mmol), KH (92 mg, 2.3 mmol), $TiCl_3(THF)_3$ (0.353 g, 0.952 mmol), yield 50 % brown solid (0.29 g, 0.48 mmol). MS(EI): *m/z* = 604.3 ($M^{+\cdot}$, 15 %), 585.2 ($[M^+–2Me]^+$, 50 %), 556.2 ($[M^+–Me–Cl]^+$, 100%); Analysis. Found: C, 63.48; H, 5.78; N, 11.52; $C_{32}H_{35}ClN_5O_2Ti$ requires: C, 63.53; H, 5.83; N, 11.58 %; IR (nujol, KBr): ν 1574 (C=N), 1500 cm^{-1} (C=C).

$VCl(L^P)$: H_2L^P (0.40 g, 0.67 mmol), KH (80 mg, 2 mmol), $VCl_3(THF)_3$ (0.251g, 0.67 mmol), yield 61 % red solid (0.28 g, 0.41 mmol). Crystals of $VCl(OH_2)(L^P)$ suitable for X-ray crystallography were grown by hexane diffusion into a THF solution of $VCl(L^P)$. MS(EI): *m/z* = 683.5 (M^+, 4 %, 634.1 ($[M^+–Cl–Me]^+$, 100 %); Analysis. Found: C, 61.39; H, 5.99; N, 8.15; $C_{35}H_{40}ClN_4O_5V$ requires: C, 61.54; H, 5.90; N, 8.20 %; IR (nujol, KBr): ν 1566 (C=N), 1507 cm^{-1} (C=C).

Crystallographic issues: Hydrogen atoms on the water molecule O100 were located in the difference Fourier map and refined at fixed distances with riding thermal parameters.

$VCl(L^{NMe})$: H_2L^{NMe} (0.497 g, 0.949 mmol), KH (0.114 g, 2.85 mmol), $VCl_3(THF)_3$ (0.355 g, 0.949 mmol), yield 54 % red solid (0.31 g, 0.51 mmol). MS(EI): *m/z* = 607.1 (M^+, 5 %), 588.2 ($[M^+–Cl+O]^+$, 100 %), 572.2 ($[M^+–Cl]^+$, 85 %); Analysis. Found: C, 63.30; H, 5.96; N, 11.42; $C_{32}H_{35}ClN_5O_2V$ requires: C, 63.21; H, 5.80; N, 11.52 %; IR (nujol, KBr): ν 1564 (C=N), 1500 cm^{-1} (C=C).

$CrCl(Lf^{NMe})$: A mixture of H_2Lf^{NMe} (0.119 g, 0.19 mmol) and KH (30 mg, 0.75 mmol) was treated with THF (7 mL) and stirred until effervescence had ceased. The red solution was filtered onto a stirring solution of $CrCl_3(THF)_3$ (0.1438 g, 0.384 mmol) and stirred for 4 h. The solvent was removed under vacuum and the red solid extracted with toluene (10 mL), filtered, and the filtrate evaporated to dryness to yield $CrCl(Lf^{NMe})$ as a red solid (0.094 g, 0.13 mmol, 69 %). Crystals of $CrCl(OH_2)(Lf^{NMe})$ suitable for X-ray crystallography were grown by C_6D_6 diffusion into a $CDCl_3$ solution of $CrCl(Lf^{NMe})$. Analysis. Found: C, 68.20; H, 4.89; N, 8.79; $C_{44}H_{41}ClN_5O_3$ requires: C, 68.17; H, 5.33; N, 9.03 %; IR (nujol, KBr): ν 1572 (C=N), 1504 cm^{-1} (C=C).

Crystallographic issues: The crystals were small and weakly diffracting, and were collected using a Cu source but only out to 1 Å.

Cobalt complexes

Co(L^{NMe}): A mixture of H_2L^{NMe} (0.231 g, 0.441 mmol) and excess KH (53 mg, 1.32 mmol) was treated with THF (15 mL). Gas evolved immediately, and, once effervescence had ceased, the mixture was filtered onto a stirring suspension of $CoCl_2$ (57 mg, 0.44 mmol) in THF (10 mL) at -80 °C. A rapid colour change from red to very dark red was observed and the reaction warmed to room temperature and left to stir overnight after which it was filtered and solvents removed under vacuum giving Co(L^{NMe}) as a red solid (0.153g, 0.265 mmol, 60%). Crystals of [Co_2($^{2+2}L^{NMe}$)] were grown by hexane diffusion into a THF solution of Co(L^{NMe}). ^{1}H NMR (399.90 MHz, C_6D_6): δ 72.01 (s, 2H), 44.51 (s, 2H), 24.34 (s, 2H), -3.77 (s, 2H), -4.74 (s, 3H), -10.07 (s, 2H), -11.35 (s, 2H), -13.40 (s, 3H), -20.44 (s, 2H), -21.78 (s, 5H, (3H + 2H), -24.23 (s, 2H), -28.29 – -34.00 (m, 6H (3 × 2H)), -43.33 (s, 2H); MS(EI): *m/z* = 580.2 (M^+, 40 %), 551.2 ([M^+–Et]$^+$, 100%); Analysis. Found: C, 66.13; H, 5.98; N, 12.10; $C_{32}H_{35}CoN_5O_2$ requires: C, 66.20; H, 6.08; N, 12.06 %; IR (nujol, KBr): ν 1565 (C=N), 1500 cm^{-1} (C=C).

Co(L^{NMes}): H_2L^{NMes} (0.190 g, 0.298 mmol), KH (0.070 g, 1.78 mmol), $CoCl_2$ (0.039g, 0.298 mmol), yield 75 % red solid (0.153 g, 2.23 mmol). ^{1}H NMR (599.81 MHz, C_6D_6): δ 73.63 (2H), 45.37 (2H), 3.68 (3H), 2.19 (2H), 1.53 (2H), 0.44 (3H), -0.12 (3H), -3.38 (2H), -3.92 (2H), -5.41 (2H), -5.73 (2H), -8.35 (2H), -9.09 (2H), -14.21 (2H), -14.75 (2H), -20.19 (1H), -22.78 (1H), -30.16 (3H), -33.01 (3H), -42.96 (2H); Analysis. Found: C, 70.00; H, 6.21; N, 10.15; $C_{40}H_{43}N_5O_2Co$ requires: C, 70.16; H, 6.33; N, 10.23 %; MS(EI): *m/z* = 684.2(M^+, 41%); IR (KBr, nujol): ν 1558 (C=N), 1499 cm^{-1} (C=C).

Co(Lf^P): H_2Lf^P (0.215 g, 0.310 mmol), KH (37 mg, 0.931 mmol), yield 19 % red solid (45 mg, 0.060 mmol). ^{1}H NMR (399.90 MHz, C_6D_6): δ 60.04 (s, 2H), 35.53 (s, 2H), 12.83 (s, 2H), 4.65 (s, 2H), 3.21 (s, 1H), 2.88 (t, *J* = 7.3 Hz, 1H), 2.76 (d, *J* = 8.1 Hz, 1H), 2.51 (d, *J* = 8.0 Hz, 1H), 1.35 (s, 2H), 1.20 (s, 4H), 0.60 (s, 2H), -1.17 (d, *J* = 6.3 Hz, 1H), -1.43 (s, 1H), -1.57 (s, 1H), -2.86 (s, 2H), -3.72 (s, 2H), -5.35 (s, 2H), -9.22 (s, 2H), -12.00 (s, 2H), -18.74 (s, 2H), -22.85 (s, 1H), -37.06 (s, 2H); MS(EI): *m/z* = 749.2 (M^+, 100%); IR (nujol, KBr): ν 1562 (C=N), 1502 cm^{-1} (C=C).

Co(Lf^{NMe}): H_2Lf^{NMe} (0.195 g, 0.316 mmol), KH (38 mg, 0.95 mmol), $CoCl_2$ (41 mg, 0.316 mmol), yield 23 % red solid (50 mg, 0.074 mmol). ^{1}H NMR (399.90 MHz, H_8-THF/C_6D_6): δ 44.61 (s, 2H), 26.05 (s, 2H), 11.49 (s, 1H), 9.71 (s, 1H), 7.79 (s, 2H), 6.68 (s, 2H), 5.89 (s, 2H), 5.61 (s, 1H), 4.30 (s, 2H), 0.83 (s, 1H), -0.84 (s, 3H), -1.77–-2.50 (m, 2 × 1H), -3.26 (s, 1H), -5.15 (s, 2H), -6.29 (s, 2H), -6.89 (s, 2H), -8.66 (s, 2H), -14.07 (s, 1H), -17.19 (s, 2H). MS(EI): *m/z* = 674.3 (M^+, 100 %); Analysis. Found: C, 71.18; H, 4.84; N, 10.29; $C_{40}H_{33}CoN_5O_2$ requires: C, 71.21; H, 4.93; N, 10.38 %; IR (nujol, KBr): ν 1560 (C=N), 1495 cm^{-1} (C=C).

Crystallographic issues: The hydrogen atoms on the water molecule were located in the difference Fourier map and refined at fixed bond distances with riding thermal parameters.

$Co(OH_2)(OH)(Lf^P)$: A solution of $Co(Lf^P)$ (0.201 g, 0.268 mmol) in air-saturated THF (8 mL) was left to stand exposed to air overnight during which a brown/red precipitate formed. This was isolated by filtration and dried under vacuum giving $Co(OH_2)(OH)(Lf^P)$ as a red/brown solid (0.179 g, 0.228 mmol, 85 %). Crystals of $Co(OH_2)(OH)(Lf^P)$ suitable for X-ray diffraction were grown from an air-saturated toluene solution of $Co(Lf^P)$. ^{1}H NMR (399.90 MHz, C_6D_6): δ 7.78–7.71 (m, *J* = 5.8 Hz, 2H, Ar-H), 7.53–7.45 (m, 1H, Ar-H), 7.43 (s, 2H, imine), 7.40–7.31 (m, *J* = 6.2 Hz, 2H, Ar-H), 7.28–7.21 (m, 2H, Ar-H), 7.12–7.05 (m, 3H, Ar-H), 6.93–6.82 (m, 4H, pyrrole + Ar-H), 6.58–6.50 (m, 2H, Ar-H), 6.25–6.18 (m, 2H, Ar-H), 6.01 (s, 2H, pyrrole), 3.48–2.72 (m, 16H, OCH_2); $^{13}C\{^1H\}$ NMR (125.76 MHz, C_6D_6): δ 162.88 (s, CH, imine), 151.20 (s, quaternary), 149.43 (s, quaternary), 139.94 (s, quaternary), 133.38 (s, quaternary), 128.61 (s, quaternary), 125.72 (s, quaternary), 125.47 (s, quaternary) 121.77 (s, CH), 121.63 (s, CH, Ar-H), 121.28 (s, CH, Ar-H), 120.84 (s, CH, Ar-H), 120.52 (s, CH, Ar-H), 120.19 (s, quaternary), 119.64 (s, CH, Ar-H), 118.76 (s, CH, Ar-H), 117.53 (s, CH, Ar-H), 117.28 (s, CH, Ar-H), 115.07 (s, CH, Ar-H), 111.57 (s, CH, Ar-H), 111.45 (s, CH, pyrrole), 107.93 (s, CH, Ar-H), 106.27 (s, CH, pyrrole), 73.00 (s, CH_2, OCH_2), 70.36 (s, CH_2, OCH_2), 70.12 (s, CH_2, OCH_2), 68.64 (s, CH_2, OCH_2) 57.53 (s, quaternary); Analysis. Found: C, 65.90.; H, 5.34; N, 7.11; $C_{43}H_{41}CoN_4O_7$ requires: C, 65.81; H, 5.27; N, 7.14 %; IR (KBr): ν 3409 (O-H), 3232 (O-H), 1564 (C=N), 1500 cm^{-1} (C=C).

Crystallographic issues: The crystals were poorly diffracting. We were unable to model disordered solvent satisfactorily, so the SQUEEZE routine of PLATON[55] was used and accounted for 11 electrons in 1608 $Å^3$, suggesting the presence of four molecules of water in the unit cell.

Manganese and iron complexes

$Mn(L^P)$: A mixture of H_2L^P (0.412 g, 0.688 mmol) and excess KH (83 mg, 2.1 mmol) was treated with THF (15 mL). Gas evolved immediately, and, once effervescence had ceased, the mixture was filtered onto a stirring suspension of $MnCl_2$ (86.5 mg, 0.688 mmol) in THF (10 mL) at -80 °C. A rapid colour change from red to very dark red was observed and the reaction warmed to room temperature and left to stir overnight after which it was filtered and solvents removed under vacuum giving $Mn(L^P)$ as a red solid (0.282 g, 0.433 mmol, 63 %). Crystals of $Mn_2(^{2+2}L^P)$ were grown by hexane diffusion into a THF solution of $Mn(L^P)$. MS(EI): *m/z* = 651.2 (M^+, 20 %), 622.1 ($[M^+–Et]^+$, 100 %); Analysis. Found: C, 64.40; H, 6.27; N, 8.48; $C_{35}H_{40}MnN_4O_5$ requires: C, 64.51; H, 6.19; N, 8.60 %; IR (nujol, KBr): ν 1562 (C=N), 1507 cm^{-1}(C=C).

$Mn(L^{NMe})$: H_2L^{NMe} (0.507 g, 0.968 mmol), KH (0.116 g, 2.9 mmol), $MnCl_2$ (0.122 mg, 0.968 mmol), yield 40 % red solid (0.223 g, 0.387 mmol). MS(EI) *m/z* = 577.1 (M^+, 20 %), 489.1 ($[M^+–(O_2(CH_2)_4NMe)]^+$, 100 %); Analysis. Found: C, 66.55; H, 6.22; N, 12.04; $C_{32}H_{35}N_5O_2Mn$ requires: C, 66.66; H, 6.12; N, 12.15 %; IR

(nujol, KBr): ν 1566 (C=N), 1507 cm^{-1} (C=C).

Fe(L^P): H_2L^P (0.387 g, 0.646 mmol), KH (78 mg, 1.94 mmol), $FeBr_2.THF_2$ (0.232 mg, 0.646 mmol), yield 62 % red solid (0.262 g, 0.40 mmol). Crystals of $Fe_2(^{2+2}L^P)$ were grown by hexane diffusion into a THF solution of Fe(L^P). ^{1}H NMR (399.90 MHz, C_6D_6): δ 36.66 (s, 2H), 35.21 (s, 2H), 30.55 (s, 2H), 24.58 (s, 2H), 23.84 (s, 2H), 12.12 (s, 2H), 9.91 (s, 2H), 9.20 (s, 2H), 1.41–1.16 (m, 4H), 0.99–0.71 (m, 3H), -2.41 (s, 3H), -4.72 (s, 2H), -6.81 (s, 2H), -10.81 (s, 4H), -11.89 (s, 2H), -14.72 (s, 4H). MS(EI): *m/z* = 652.2 (M^+, 100%), 624.2 ($[M^+–Et]^+$, 89%); IR (Nujol, KBr): ν 1559 (C=N), 1507 cm^{-1}(C=C).

Crystallographic issues: Attempts to model a disordered benzene molecule were unsuccessful and led to a diverging solution, so these atoms were refined using isotropic approximation restraints.

Conclusions

In order to overcome problems associated with the formation of mononuclear instead of binuclear Pacman complexes of the symmetrical Schiff-base pyrrole macrocycle H_4L, yet retain its features that enable the control of both primary and secondary coordination environments, we prepared a series of heteroditopic compartmental macrocycles that separate, through aryl spacers, a pyrrole-imine N_4 donor set from alternative O_5 or ONO donors. These new macrocycles were straightforwardly prepared in good yields from easily accessed starting materials, and displayed similar hydrogen bond donor-acceptor properties to their symmetrical congeners. Furthermore, in the majority of cases, metallation of these macrocycles resulted in the formation of mononuclear complexes that adopt Pacman-like, cleft structures in which the O_5 or ONO donor sets remained vacant and oriented above the axial metal site. It is clear that this relatively rigid assembly facilitates the bonding of guest molecules, in particular water, through both coordination to the metal and through hydrogen-bonding interactions to the O and N acceptors of the second pocket, and should therefore be able to stabilise potentially reactive intermediates that are formed during redox reactions. It is also possible that the fluorenyl substituent at the *meso* carbon can hydrogen bond to axial substituents and be part of a defining reaction pocket constructed from the ligand periphery. In some instances, the flexibility of the larger O_5 donor set resulted in the formation of potassium helicates instead of the expected Pacman geometries, and also direct O-Ti bond formation with the more oxophilic Ti centre, so it is anticipated that the smaller, more rigid ONO donor set will be more exploitable in the evaluation of the reaction chemistry of these systems. The presence of a small quantity of [2+2] cyclised product was inferred from NMR and MS data, and also from the preferential crystallisation of binuclear Fe, Mn, and Co helicates. While this macrocycle is only present in low yield, it is clear that new synthetic strategies are required that favour the sole formation of either [1+1] or [2+2] macrocycles, especially as these ligand variants offer very different structural and functional aspects to their complexes.

Notes and references

[1] R. L. Shook and A. S. Borovik, *Chem. Commun.*, 2008, 6095.

[2] S. Fukuzumi, *Chem. Lett.*, 2008, **37**, 808.

[3] S. Y. Reece and D. G. Nocera, *Annu. Rev. Biochem.*, 2009, **78**, 673; P. W. N. M. van Leeuwen, *Supramolecular catalysis*, Wiley-VCH, Weinheim, 2008; T. S. Koblenz, J. Wassenaar and J. N. H. Reek, *Chem. Soc. Rev.*, 2008, **37**, 247; B. Breit, *Angew. Chem. Int. Ed.*, 2005, **44**, 6816.

[4] A. L. Gavrilova and B. Bosnich, *Chem. Rev.*, 2004, **104**, 349.

[5] C. Finn, S. Schnittger, L. J. Yellowlees and J. B. Love, *Chem. Commun.*, 2012, **48**, 1392; M. L. Rigsby, S. Mandal, W. Nam, L. C. Spencer, A. Llobet and S. S. Stahl, *Chem. Sci.*, 2012, **3**, 3058; V. Artero, M. Chavarot-Kerlidou and M. Fontecave, *Angew. Chem. Int. Ed.*, 2011, **50**, 7238; T. S. Teets and D. G. Nocera, *Chem. Commun.*, 2011, **47**, 9268; A. A. Gewirth and M. S. Thorum, *Inorg. Chem.*, 2010, **49**, 3557; E. E. Benson, C. P. Kubiak, A. J. Sathrum and J. M. Smieja, *Chem. Soc. Rev.*, 2009, **38**, 89; J. L. Dempsey, A. J. Esswein, D. R. Manke, J. Rosenthal, J. D. Soper and D. G. Nocera, *Inorg. Chem.*, 2005, **44**, 6879.

[6] G. Thiabaud, G. Guillemot, I. Schmitz-Alfonso, B. Colasson and O. Reinaud, *Angew. Chem. Int. Ed.*, 2009, **48**, 7383; C. Jeunesse, D. Armspach and D. Matt, *Chem. Commun.*, 2005, 5603; D. V. Yandulov and R. R. Schrock, *Science*, 2003, **301**, 76.

[7] P. D. Harvey, C. Stern, C. P. Gros and R. Guilard, *Coord. Chem. Rev.*, 2007, **251**, 401.

[8] J. Rosenthal and D. G. Nocera, *Acc. Chem. Res*, 2007, **40**, 543; J. P. Collman, P. S. Wagenknecht and J. E. Hutchinson, *Angew. Chem. Int. Ed.*, 1994, **33**, 1537.

[9] J. P. Collman, R. Boulatov, C. J. Sunderland and L. Fu, *Chem. Rev.*, 2004, **104**, 561.

[10] R. McGuire Jr, D. K. Dogutan, T. S. Teets, J. Suntivich, Y. Shao-Horn and D. G. Nocera, *Chem. Sci.*, 2010, **1**, 411.

[11] I. Hijazi, T. Roisnel, M. Fourmigué, J. Weiss and B. Boitrel, *Inorg. Chem.*, 2010, **49**, 3098; D. Natale and J. C. Mareque-Rivas, *Chem. Commun.*, 2008, 425; J. D. Soper, S. V. Kryatov, E. V. Rybak-Akimova and D. G. Nocera, *J. Am. Chem. Soc.* , 2007, **129**, 5069; J. Rosenthal and D. G. Nocera, *Prog. Inorg. Chem.*, 2007, **55**, 483; L. L. Chng, C. J. Chang and D. G. Nocera, *Org. Lett.*, 2003, **5**, 2421; C. J. Chang, L. L. Chng and D. G. Nocera, *J. Am. Chem. Soc.*, 2003, **125**, 1866; J. P. Collman, L. Fu, P. C. Herrmann and X. Zhang, *Science*, 1997, **275**, 949.

[12] J. P. Collman, *Acc. Chem. Res.*, 1977, **10**, 265; J. P. Collman, N. K. Devaraj, R. A. Decréau, Y. Yang, Y.-L. Yan, W. Ebina, T. A. Eberspacher and C. E. D. Chidsey, *Science*, 2007, **315**, 1565.

[13] P. Even and B. Boitrel, *Coord. Chem. Rev.*, 2006, **250**, 519.

[14] J. B. Love, *Chem. Commun.*, 2009, 3154

[15] G. Givaja, A. J. Blake, C. Wilson, M. Schröder and J. B. Love, *Chem. Commun.*, 2003, 2508.

[16] J. L. Sessler, W.-S. Cho, S. P. Dudek, L. Hicks, V. M. Lynch and M. T. Huggins, *J. Porphyrins Phthalocyanines*, 2003, **7**, 97; W. B. Callaway, J. M. Veauthier and J. L. Sessler, *J. Porphyrins Phthalocyanines*, 2004, **8**, 1.

[17] E. Askarizadeh, S. Bani Yaghoob, D. M. Boghaei, A. M. Z. Slawin and J. B. Love, *Chem. Commun.*, 2010, **46**, 710.

[18] A. M. J. Devoille and J. B. Love, *Dalton Trans.*, 2012, **41**, 65.

[19] P. L. Arnold, D. Patel, A. J. Blake, C. Wilson and J. B. Love, *J. Am. Chem. Soc.*, 2006, **128**, 9610; P. L. Arnold, D. Patel, C. Wilson and J. B. Love, *Nature*, 2008, **451**, 315; P. L. Arnold, G. M. Jones, S. O. Odoh, G. Schreckenbach, N. Magnani and J. B. Love, *Nat. Chem.*, 2012, **4**, 221; P. L. Arnold, E. Hollis, F. J. White, N. Magnani, R. Caciuffo and J. B. Love, *Angew. Chem., Int. Ed.*, 2011, **50**, 887; P. L. Arnold, A.-F. Pécharman and J. B. Love, *Angew. Chem. Int. Ed.*, 2011, **50**, 9456; P. L. Arnold, D. Patel, A. F. Pécharman, C. Wilson and J. B. Love, *Dalton Trans.*, 2010, **39**, 3501; P. L. Arnold, J. B. Love and D. Patel, *Coord. Chem. Rev.*, 2009, **253**, 1973.

[20] J. W. Leeland, A. M. Z. Slawin and J. B. Love, *Organometallics*, 2010, **29**, 714.

[21] J. W. Leeland, F. J. White and J. B. Love, *Chem. Commun.*, 2011, **47**, 4132.

[22] G. Givaja, M. Volpe, J. W. Leeland, M. A. Edwards, T. K. Young, S. B. Darby, S. D. Reid, A. J. Blake, C. Wilson, J. Wolowska, E. J. L. McInnes, M. Schröder and J. B. Love, *Chem. Eur. J.*, 2007, **13**, 3707.

[23] E. Askarizadeh, A. M. J. Devoille, D. M. Boghaei, A. M. Z. Slawin and J. B. Love, *Inorg. Chem.*, 2009, **48**, 7491.

[24] M. Volpe, S. D. Reid, A. J. Blake, C. Wilson and J. B. Love, *Inorg. Chim. Acta*, 2007, **360**, 273.

[25] J. Arnold, D. Y. Dawson and C. G. Hoffman, *J. Am. Chem. Soc.*, 1993, **115**, 2707.

[26] S. D. Reid, A. J. Blake, C. Wilson and J. B. Love, *Inorg. Chem.*, 2006, **45**, 636.

[27] M. Tayebani, S. Conoci, K. Feghali, S. Gambarotta and G. P. A. Yap, *Organometallics*, 2000, **19**, 4568.

[28] S.-Z. Fu, D.-Q. Wang and J.-M. Dou, *Acta Cryst., E*, 2007, **63**, m1522; M. J. Zaworotko, C. R. Kerr and J. L. Atwood, *Organometallics*, 1985, **4**, 238; J.-M. Lu, S. V. Rosokha, S. V. Lindeman, I. S. Neretin and J. K. Kochi, *J. Am. Chem. Soc.*, 2005, **127**, 1797.

[29] A. F. Richards, M. Brynda and P. P. Power, *J. Am. Chem. Soc.*, 2004, **126**, 10530; P. B. Hitchcock, M. F. Lappert, G. A. Lawless and B. Royo, *J. Chem. Soc., Chem. Commun.*, 1993, 554.

[30] J. M. Veauthier, W.-S. Cho, V. M. Lynch and J. L. Sessler, *Inorg. Chem.*, 2004, **43**, 1220.

[31] S. J. Coles, M. B. Hursthouse, D. G. Kelly, A. J. Toner and N. M. Walker, *J. Organomet. Chem.*, 1999, **580**, 304; M. Pasquali, F. Marchetti, A. Landi and C. Floriani, *J. Chem. Soc., Dalton Trans.*, 1978, 545.

[32] R. Crescenzi, E. Solari, C. Floriani, A. Chiesi-Villa and C. Rizzoli, *Organometallics*, 1996, **15**, 5456; A. Spannenberg, V. V. Burlakov, P. Arndt, M. Klahn and U. Rosenthal, *Z. Kristallogr.-New Cryst. Struct*, 2007, **222**, 192.

[33] D. G. Sekutowski and G. D. Stucky, *Inorg. Chem.*, 1975, **14**, 2192; T. Matsuo, H. Kawaguchi and M. Sakai, *J. Chem. Soc., Dalton Trans.*, 2002, 2536.

[34] M. Talja, M. Klinga, M. Polamo, E. Aitola and M. Leskelä, *Inorg. Chim. Acta*, 2005, **358**, 1061; M. Mazzanti, J.-M. Rosset, C. Floriani, A. Chiesi-Villa and C. Guastini, *J. Chem. Soc., Dalton Trans.*, 1989, 953.

[35] K. Yamamoto, K. Oyaizu and E. Tsuchida, *J. Am. Chem. Soc.*, 1996, **118**, 12665; J.-Q. Wu, L. Pan, N.-H. Hu and Y.-S. Li, *Organometallics*, 2008, **27**, 3840.

[36] D. Reardon, F. O. Conan, S. Gambarotta, G. Yap and Q. Wang, *J. Am. Chem. Soc.*, 1999, **121**, 9318; S. Ciurli, C. Floriani, A. Chiesi-Villa and C. Guastini, *J. Chem. Soc., Chem. Commun.*, 1986, 1401.

[37] K. Ejsmont and R. Kubiak, *Acta Cryst. C*, 1998, **54**, 1844; D. Reardon, J. Guan, S. Gambarotta, G. P. A. Yap and D. R. Wilson, *Organometallics*, 2002, **21**, 4390.

[38] M. Mazzanti, C. Floriani, A. Chiesi-Villa and C. Guastini, *Inorg. Chem.*, 1986, **25**, 4158; D. G. McCollum, G. P. A. Yap, L. Liable-Sands, A. L. Rheingold and B. Bosnich, *Inorg. Chem.*, 1997, **36**, 2230.

[39] P. L. Arnold, A. J. Blake, C. Wilson and J. B. Love, *Inorg. Chem.*, 2004, **43**, 8206.

[40] N. S. Dean, L. M. Mokry, M. R. Bond, C. J. O'Connor and C. J. Carrano, *Inorg. Chem.*, 1996, **35**, 2818; M. Kosugi, S. Hikichi, M. Akita and Y. Moro-oka, *Inorg. Chem.*, 1999, **38**, 2567; J. C. Dutton, G. D. Fallon and K. S. Murray, *J. Chem. Soc., Chem. Commun.*, 1990, 64; K. Kanamori, T. Okayasu and K.

Okamoto, *Chem. Lett.*, 1995, **24**, 105; K. Kanamori, K. Yamamoto, O. Takako, N. Matsui, K. Okamoto and W. Mori, *Bull. Chem. Soc. Jpn.*, 1997, **70**, 3031.

[41] C. D. Beard, R. J. Barrie, J. Evans, W. Levason, G. Reid and M. D. Spicer, *Eur. J. Inorg. Chem.*, 2006, **2006**, 4391; C. J. Carrano, M. Mohan, S. M. Holmes, R. de la Rosa, A. Butler, J. M. Charnock and C. D. Garner, *Inorg. Chem.*, 1994, **33**, 646.

[42] M. Inamo, H. Nakaba, K. Nakajima and M. Hoshino, *Inorg. Chem.*, 2000, **39**, 4417; M. G. Basallote, P. V. Bernhardt, T. Calvet, C. E. Castillo, M. Font-Bardia, M. Martinez and C. Rodriguez, *Dalton Trans.*, 2009, 9567; R. Temple, D. A. House and W. T. Robinson, *Acta Cryst. C*, 1984, **40**, 1789.

[43] N. Kobayashi, T. Fukuda, K. Ueno and H. Ogino, *J. Am. Chem. Soc.*, 2001, **123**, 10740.

[44] H.-Y. Gong, D.-X. Wang, Q.-Y. Zheng and M.-X. Wang, *Tetrahedron*, 2009, **65**, 87; G. W. Roberts, S. C. Cummings and J. A. Cunningham, *Inorg. Chem.*, 1976, **15**, 2503.

[45] G. Givaja, M. Volpe, M. A. Edwards, A. J. Blake, C. Wilson, M. Schröder and J. B. Love, *Angew. Chem. Int. Ed.*, 2007, **46**, 584.

[46] M. Volpe, H. Hartnett, J. W. Leeland, K. Wills, M. Ogunshun, B. J. Duncombe, C. Wilson, A. J. Blake, J. McMaster and J. B. Love, *Inorg. Chem.*, 2009, **48**, 5195.

[47] S. D. Reid, A. J. Blake, W. Köckenberger, C. Wilson and J. B. Love, *Dalton Trans.*, 2003, 4387.

[48] J. P. Collman, J. L. Hoard, N. Kim, G. Lang and C. A. Reed, *J. Am. Chem. Soc.*, 1975, **97**, 2676; J. P. Battioni, I. Artaud, D. Dupre, P. Leduc, I. Akhrem, D. Mansuy, J. Fischer, R. Weiss and I. Morgenstern-Badarau, *J. Am. Chem. Soc.*, 1986, **108**, 5598.

[49] S. Ross, T. Weyhermuller, E. Bill, K. Wieghardt and P. Chaudhuri, *Inorg. Chem.*, 2001, **40**, 6656; G. J. P. Britovsek, J. England, S. K. Spitzmesser, A. J. P. White and D. J. Williams, *Dalton Trans.*, 2005, 945.

[50] S. D. Reid, C. Wilson, C. I. De Matteis and J. B. Love, *Eur. J. Inorg. Chem.*, 2007, 5286.

[51] .L. E. Manzer, *Inorg. Synth.*, 1982, **21**, 135.

[52] .C.-S. Chang, Y.-T. Lin, S.-R. Shih, C.-C. Lee, Y.-C. Lee, C.-L. Tai, S.-N. Tseng and J.-H. Chern, *J. Med. Chem.*, 2005, **48**, 3522.

[53] A. M. Skwierawska, J. F. Biernat and V. C. Kravtsov, *Tetrahedron*, 2006, **62**, 149.

[54] .L. J. Farrugia, *J. Appl. Cryst.*, 1999, **32**, 837.

[55] A. L. Spek, *Acta Crystallogr. Sect. D,* 2009*, **65,*** 148.